—Reviews—

# ナノマテリアルの有害性評価（毒性評価）

津田洋幸,[a] 徳永裕司,[b] 広瀬明彦,[c] 菅野　純*,[d]

# Hazard Identification of Nanomaterials

Hiroyuki TSUDA,[a] Hiroshi TOKUNAGA,[b] Akihiko HIROSE,[c] and Jun KANNO*,[d]

[a]*Department of Molecular Toxicology, Graduate School of Medical Sciences, Nagoya City University, 1 Kawasumi, Mizuho-cho, Mizuho-ku, Nagoya 467-8601, Japan,* [b]*Division of Environmental Chemistry,* [c]*Division of Risk Assessment, Biological Safety Research Center, and* [d]*Division of Cellular and Molecular Toxicology, Biological Safety Research Center, National Institute of Health Sciences, 1-18-1, Kamiyoga, Setagayaku, Tokyo 158-8501, Japan*

(Received July 15, 2008)

It is considered that the materials with new properties may lead to novel biological effects or unknown adverse health effects. To gather proper hazard information, it is important to develop both experimental protocols and detection/measurement methods for nanomaterials in the body, in parallel. Since 2005, we are running research projects to develop methods to monitor health risk effects for the assessment of manufactured nanomaterials funded by the Ministry of Health, Labour and Welfare. For the experimental protocols, these projects focus on the development of 1) *in vitro* experimental systems, 2) *in vivo* experimental systems (mainly focusing on long-term health implication, especially carcinogenesis), and 3) proper inhalation system. Firstly, fullerene (C60), titanium dioxide and multi-walled carbon nanotube were chosen to be tested because of their high production volume. Safety issues for new materials such as nanoparticles is a new paradigm. The key is that the full scale exposure to the public has not been started yet. Therefore, there is a good chance that information from hazard identification studies can be directly fed back to the product development plan. Manufacturers can produce safer products without risking themselves waiting for the toxicology studies to be finished after their products are widely marketed.

**Key words**——toxicity; titanium dioxide, multi-wall carbon nanotube (MWCNT); asbestos; fullerene; Absorption, Digestion, Metabolism and Exertion (ADME); carcinogenesis

ナノマテリアルは，今後の産業の新たな発展にとっての重要な新素材である．これらは，従来の素材とは異なった様々な特性を有していること，及びその有害性についても新しい問題が提起されるとの予測がなり立つことから，国民の関心を呼んでいる．しかし，これらの有害性についての研究が始まったばかりであることから，情報は少ない．Figure 1に，最近の動向を示す．2004年に産業技術総合研究所が公開フォーラムを開催し，2005年初頭に経済産業・文部科学・環境・厚生労働の4省庁関連研究所と産学が集まり「ナノテクノロジーと社会」(http://www.aist.go.jp/aist_j/research/honkaku/symposium/nanotech_society/050201/sdata.html)を開催した．これが，しばらくの間，関係各機関の連絡の場となった．

Figure 2に，現在進行中のプロジェクトを示す．厚生労働省は厚生労働科学研究費補助金（化学物質リスク研究事業）を基に，国立医薬品食品衛生研究所を中心とした研究を開始した．Figure 3に示すごとく，2004年より系統的な研究を行っている．意図的に生産されるナノマテリアルについて，人及び環境に対する有害影響の同定（有害性評価）のための研究を開始した．2004年の情報収集と研究方針出しに続き，2005年からのフラーレンや二酸化チ

[a]名古屋市立大学大学院医学研究科・分子毒性学分野（分子医学講座生体防御・総合医学専攻）（〒467-8601 名古屋市瑞穂区瑞穂町字川澄 1），[b]国立医薬品食品衛生研究所環境衛生化学部（〒158-8501 東京都世田谷区上用賀 1-18-1），現，医薬品医療機器総合機構品質管理部基準課（〒100-0013 東京都千代田区霞が関 3-3-2），[c]国立医薬品食品衛生研究所安全性生物試験研究センター総合評価研究室，[d]同毒性部（〒158-8501 東京都世田谷区上用賀 1-18-1）
*e-mail: kanno@nihs.go.jp

本総説は，日本薬学会第128年会シンポジウム S32で発表したものを中心に記述したものである．

- In 2004, the Technology Information Department of AIST launched an open forum entitled "***Nanotechnology and Society***."
- The first symposium (Feb. 2005) was organized by the four national research institutes with four different ministries.

National Institute of Advanced Industrial Science and Technology, **AIST**
National Institute for Materials Science, **NIMS**
National Institute for Environmental Studies, **NIES**
National Institute of Health Sciences, **NIHS**

***Importance of multidiscipline network***

- In 2005, the survey project of **"Research Project on Facilitation of Public Acceptance of Nanotechnology"** was conducted by the above four institutes and universities. (funded by MEXT)

➡ **Political Proposals**

In 2006, the second project of "The multidisciplinary experts panel for nanotechnology implication"
(MEXT: Ministry of Education, Culture, Sports, Science and Technology)

Fig. 1. Importance of Multidiscipline Network

**Research programmes or strategies designed to address human health and/ or environmental safety aspects of nanomaterials;**

- Ministry of Economy, Trade and Industry : (2006-2010) project
  The **NEDO** project: "Evaluation of the Potential Risks of Manufactured Nanomaterials based on Toxicity Tests with Precise Characterization."
  The project focuses on toxicity test protocols (mainly an inhalation test) and a risk assessment methodology of manufactured nanomaterials.
- Ministry of the Environment : National Institute of Environmental Sciences (**NIES**) has started a nanotoxicology programme
  - interaction of nano-fibers including CNT with cell membranes,
  - tamasepithelial and transpulmonary migration of manoparticles,
  - *in vitro* and *in vivo* toxicity assay of manomaterials

  NIES has been investigating inhalation effects of atmospheric nanoparticlesfor the last 3 years
- Ministry of Health, Labour and Welfare :The National Institution of Occupational Safety and Health (**JNIOSH**) will start a new research on possible health issues in April 2007, due to exposure to nanomaterials in the workplace.
- MHLW the Office of Chemical Safety **NIHS**

Fig. 2. Research Programmes and Strategies Designed to Address Human Health and/ or Environmental Safety Aspects of Nanomaterials

Recent research activities in NIHS granted by the "Health and Labour Sciences Research Grants" of the Office of Chemical Safety, MHLW
(Ministry of Health, Labour and Welfare)

| Fiscal year | |
|---|---|
| 2004 | Survey research of public information about health implication of nanomaterials |
| 2005 | The initial research on methodology of health risk assessment of manufactured nanomaterials started |
| 2006 (to 2008) | Restating the project of "Research on the hazard characterization and toxico-kinetic analysis of manufactured nanomaterials for the establishment of health risk assessment methodology", as the expanded project. |
| 2007 (to 2009) | "Research on the dermal toxicity evaluation methodology of the manufactured nanomaterials" |

Fig. 3. Recent Research Activities in NIHS Granted by the "Health and Labour Sciences Research Grants" of the Office of Chemical Safety, MHLW

タンを例とした測定法と有害性評価法の検討，2006年からのMWCNTを加えた長期毒性とトキシコキネティクス，ADME検討法の確立，*in vitro* 法の検討，さらに，2007年からの皮膚毒性，経皮毒性，経気道毒性を加えて，長期毒性に焦点を当てた総合的な有害性評価を開始している．

現在，手元にある意図的生産品としてのナノマテリアルは，凝集体として，あるいは，それ個有のサイズ分布の広範性により（サイズによる厳密な分画が行われていないバルク剤），マイクロメーターの次元を持つ粒子から，ナノメーターの次元を持つ粒子までが混在したものが一般的である．フラーレンはその溶媒の条件により，数百マイクロメーター大の粒子から，完全な単分子状態，さらに，溶解条件の変動により，石英状の柱状-アスベスト様の棒状の凝集体（ウィスカー）に再凝集する性質がある．このような，溶解環境の変化は，生体内では親水性（気管・気管支内，内消化管内，血液内），親油性（細胞膜など，脂質二重膜内），あるいは酸化的環境（炎症細胞による攻撃），その他，酵素的な環境を含め，複雑であることから，Fig. 4に示すごとく，体内への吸収と分布，蓄積と再分解，再分布といった複雑な動態が予測される．蓄積場所についても，血行性，リンパ行性といった移動媒体を使って脳をはじめとする全身臓器に運ばれることが想定され，または報告されている．主な排出経路としては腸管と腎が想定されるが，胆汁への移行，腎糸球体の基底膜親和性・透過性など，不明なことが多い．

実験に用いたMWCNTについては，東京都健康安全研究センターとの共同で電子顕微鏡によるサイズ，及びICP-MS等による金属等の元素含有量の測定を行った（Fig. 5）．径は約100 nmが中心で，長さは5 μm以上のものが約1/4を占めているMWCNTであった．鉄の含有量は3,500 ppmであり，以下ハロゲンや硫黄が認められた．

*In vivo* 毒性試験として，いくつかの試みを実施しているので，それらについて簡単に述べる．まず二酸化チタンの皮膚発がんプロモーション作用について，ヒトc-Ha-ras導入ラットを用いた検討を紹介する（Fig. 6）．ジメチルベンツアントラセン（DMBA）を1回塗布し，30週間，二酸化チタンを塗布した．陽性対象には皮膚発がん促進作用の知られるフォルボールエステル（TPA）[1]を，陰性対象

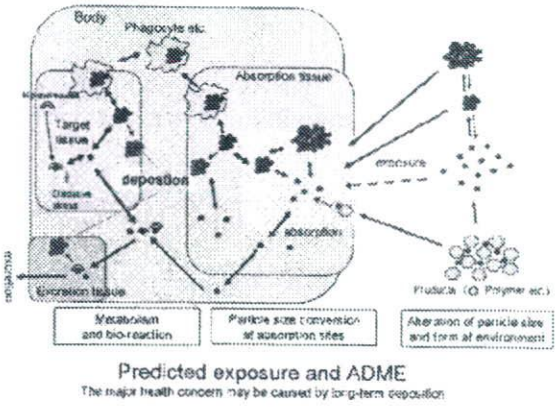


Fig. 4. Predicted Exposure and ADME

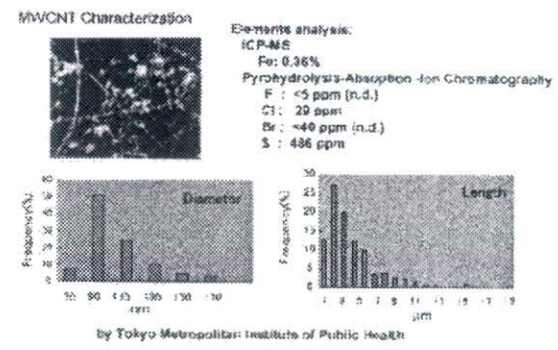


Fig. 5. Development of CNT Detection Method in the Biological Samples

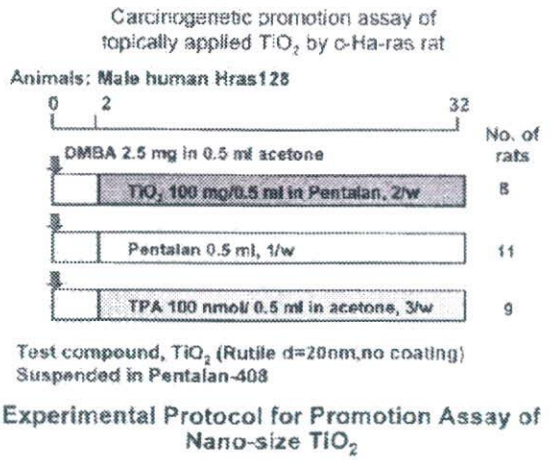


Fig. 6. Carcinogenetic Promotion Assay of Topically Applied $TiO_2$ by c-Ha-ras Rat

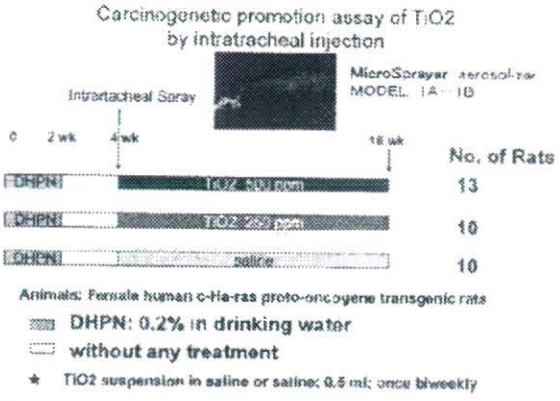


Fig. 7. Carcinogenetic Promotion Assay of $TiO_2$ by Intratracheal Injection

には懸濁溶媒（Pentalan）を用いた．その結果，二酸化チタンは皮膚乳頭腫の発生を促進する結果を得ている（投稿準備中）．

次に，気管内投与による肺発がん促進作用を同様のラットを用いて検討した（Fig. 7）．ジヒドロキシプロピルニトロサミン（DHPN）を2週間飲水投与したのち，隔週で二酸化チタンの懸濁液を気管内スプレーにて，12週間投与した．その結果，肺の過形成病変（前駆病変と考えられる）及び肺腺腫の発がん促進が認められた（投稿準備中）．フラーレンについても同様の実験が進行中である．

最後に，p53ヘテロ欠失マウスの腹腔内投与モデルを用いてのMWCNTのアスベスト様中皮腫発がん性を検討した実験を示す．陽性対象には青アスベスト（Crocidolite）を用いた．フラーレンを非ファイバー状炭素系マテリアルとしての対照に置いた（Fig. 8）．まず，腹腔内投与法の位置付けであるが，アスベスト及び代替繊維，特にグラスファイバーを用いた1970–80年代頃の多くの研究[2–4]の結果からFig. 9に示すごとく，2005年のWHO会合[5]においてもその有効性が認められている．われわれが毒性影響を検討しているMWCNTは，前述のごとく，5 μmよりも長い繊維状あるいは棒状の粒子を含んでいる．これは，もしも十分に頑丈で生体内に長期に渡り分解されずに残留した場合，1978年のPott[6]の「繊維の発がん因子」に当てはめると，Fig. 10の上段左の灰色で示した長方形の領域に当たる繊維をこのMWCNTが含んでいることが分り，当然の帰結として，アスベスト様発がん作用

を有していることが予測される．上段右に示すように，アスベストのp53ヘテロ欠失マウスの腹腔内投与は，野生型マウスにおける中皮腫発がんの期間を短縮することがKaneらのグループにより示されている．[7][8]

用量の設定については，M. Rollerらの論文[9]にあるように（Fig. 11）中皮腫発がん性の弱い繊維の検出が可能な腹腔内投与量が$10^9$～$10^{10}$本であることを参考に設定した．この本数で陰性であれば問題ないことになるとの考えである．この実験の結果はFig. 12に示すように，MWCNTが青アスベストと同等の中皮腫発がん性を持つことが示された[10]．なお，体内滞留時間が長いチタン酸カリウムウィスカー，炭化ケイ素ウィスカー，酸化チタンウィスカーはいずれもラット腹腔内投与による中皮腫発がんが知られている．[11]

ナノマテリアルの有害性評価は，ヒトへの大掛かりな暴露が始まっていない現在，製造者側への安全な製品開発に必要な情報提供としての意味合いが大

Asbestos-like fiber carcinogenesis assay of MWCNT
by intraperitoneal administration to p53+/- mouse

Experimental Design

| | | |
|---|---|---|
| ・animal | p53+/- mouse (C57BL/6 back, 9 - 11weeks age) | |
| | 4 groups (18 - 19 per group) | |
| ・administration | single intraperitoneal administration | |
| | 1. MWCNT | 3mg/animal = 1x10⁹ fiber/animal |
| | 2. fullerene | 3mg/animal |
| | 3. crocidolite | 3mg/animal = 1x10¹⁰ fiber/animal |
| | 4. vehicle | |
| ・sample preparation: suspended in 0.5%CMC solution, autoclaved, added tween 80 (1%), and sonicated | | |

Fig. 8. Asbestos-like Fiber Carcinogenesis Assay of MWCNT by Intraperitoneal Administration to p53+/− Mouse

**WHO Workshop on Mechanisms of Fibre Carcinogenesis and Assessment of Chrysotile Asbestos Substitutes**
8-12 November 2005, Lyon, France "SUMMARY CONSENSUS REPORT"

- **Methodological Aspects**

Epidemiologic studies
a clear advantage, but does not always override contrary findings from toxicological studies

In in vivo animal studies,
- carcinogenic response (lung cancer, mesothelioma) and fibrosis were considered to be the key effects;
- epithelial cell proliferation, and inflammation were not regarded to be equally important indicators
- the sensitivity of lung tumors in the rat is clearly lower than that in humans. (reason is still unclear)
- **testing of fibres by intraperitoneal injection represents a useful and sensitive assay.**

Fig. 9. WHO Workshop on Mechanisms of Fibre Carcinogenesis and Assessment of Chrysotile Asbestos Substitutes

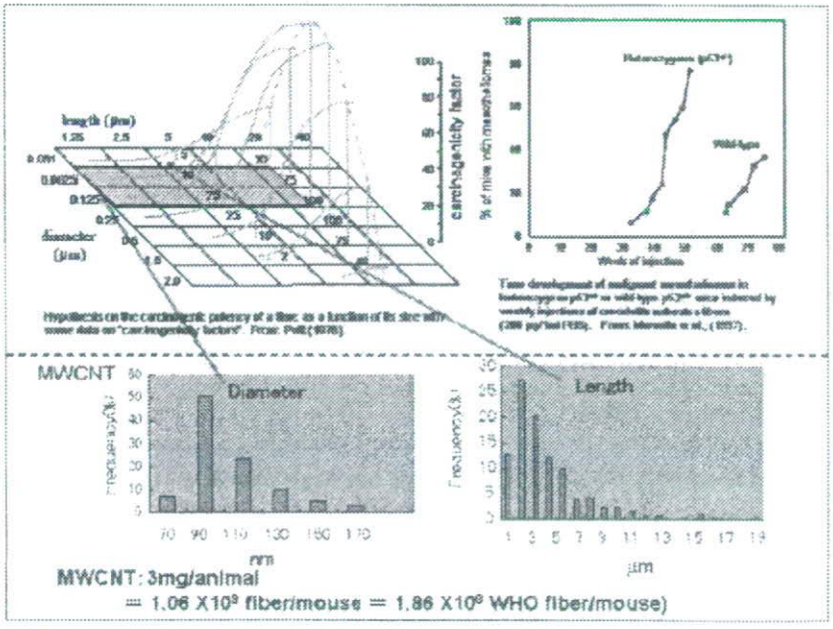


Fig. 10. MWCNT, Its Size and Property

きい．今までの新素材の中には，慢性毒性情報の乏しいことが「低毒性」であることと誤解され，数十年の歳月を掛けて国民的人体実験の結果として中皮腫発がんが顕在化した例がある．国を挙げての新技術開発を担うナノマテリアルは，少なくとも既知の科学的根拠に依拠した有害性によって未来に汚点を残すことだけは，その中長期的経済発展の観点からも，国民の安全の立場からも，避けなければならない．

MWCNT の中皮腫誘発性の問題は，これから検討されるべきナノサイズの粒子の有害性同定（毒性評価）とは別のものである[12-17]．言い換えると，本当のナノサイズの粒子そのものの有害性同定は始まったばかりであり，毒性学の今後の大きな課題である．細胞内の酵素などのタンパク質分子とほとんど同じサイズのナノマテリアルの毒性メカニズムは，今までの毒性学の常識では同定・解析できない可能性もある．最先端の分子毒性学との連携が必須の要因となることが想定される．今後の安全性確保体制の強化には，不足する毒性学研究者の補充と育成も急務である．

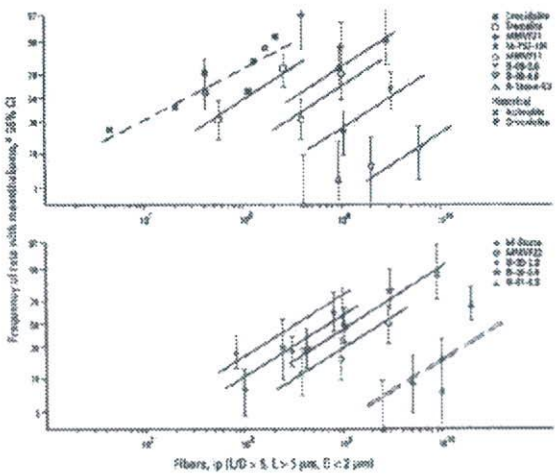

Fig. 11. Fiber Mesotheliomagenesis, Comparative Data among Various Fibrous Amterials

## REFERENCES


1) Park C. B., Fukamachi K., Takasuka N., Han B. S., Kim C. K., Hamaguchi T, Fujita K, Ueda S, Tsuda H., *Cancer Sci. Mar.*, 95(3): 205–210 (2004).
2) World Health Organization "Environmental Health Criteria 53. Asbestos and Other Natural Mineral Fibres." World Health Organization, Geneva (1986).
3) World Health Organization "Environmental Health Criteria 203. Chrysotile Asbestos." World Health Organization, Geneva (1986).
4) World Health Organization "Man-made vitreous fibres. IARC monographs on the evaluation of carcinogenic risk to humans.," Vol. 81, IARC Lyon (2002).


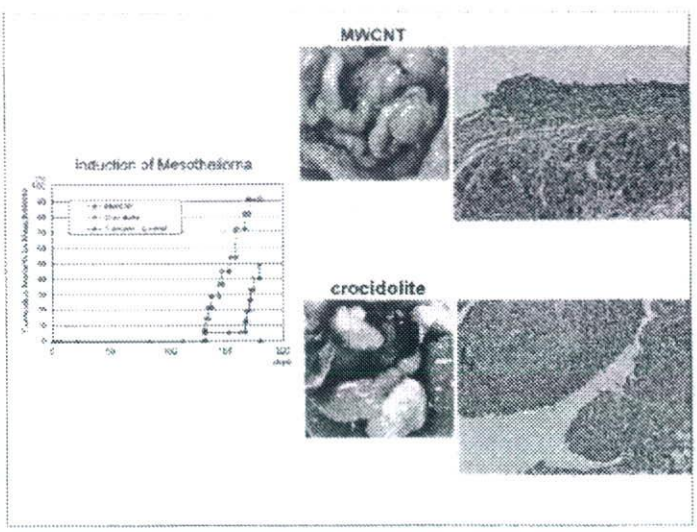


Fig. 12. Induction of Mesothelioma in p53+/− Mouse by Intraperitoneal Application of Multi-wall Carbon Nanotube

5) http://www.who.int/ipcs/publications/new_issues/summary_report.pdf
6) Pott F., Staub-Reinhalt. Luft, **38**, 486–490 (1978).
7) Marsella J. M., Liu B. L., Vaslet C. A., Kane A. B., *Health Perspect.*, **105** (Suppl. 5), 1069–1072 (1997).
8) Vaslet C. A., Messier N. J., Kane A. B., *Toxicol. Sci.*, **68**, 331–338 (2002).
9) Roller M., Pott F., Kamino K., Althoff G. H., Bellmann, B., *Environ. Health Perspect.*, **105** (Suppl. 5), 1253–1256 (1997).
10) Takagi A, Hirose A, Nishimura T, Fukumori N, Ogata A, Ohashi N, Kitajima S, Kanno J., *J, Toxicol. Sci.*, **33**(1), 105–116 (2008).
11) Adachi S., Kawamura K., Takemoto K., *Ind. Health*, **39**, 168–174 (2001).
12) Gulumian M., van Wyk J. A., *Chem. Biol. Interact.*, **62**, 89–97 (1987).
13) Moalli P. A., MacDonald J. L., Goodglick L. A., Kane A. B., *Am. J. Pathol.*, **128**, 426–445 (1987).
14) Lippmann M., *Environ. Health Perspect.*, **88**, 311–317 (1990).
15) Pott F., Roller M., Kamino K., Bellmann B., *Environ. Health Perspect.*, **102**, (Suppl. 5), 145–150 (1994).
16) Bernstein D. M., Riego Sintes J. M., *European Chemicals Bureau*, 44–45 (1999).
17) Hei T. K., Xu A., Huang S. X., Zhao Y., *Inhal. Toxicol.*, **18**, 985–990 (2006).

# Induction of a novel histone deacetylase 1/c-Myc/Mnt/Max complex formation is implicated in parity-induced refractoriness to mammary carcinogenesis

Yoichiro Matsuoka,[1,3] Katsumi Fukamachi,[2] Norihisa Uehara,[1] Hiroyuki Tsuda[2] and Airo Tsubura[1]

[1]Second Department of Pathology, Kansai Medical University, 10-15 Fumizono-cho, Moriguchi, Osaka 570-8506; [2]Department of Molecular Toxicology, Nagoya City University Graduate School of Medical Sciences, Mizuho-cho, Mizuho-ku, Nagoya 467-8601, Japan

(Received July 1, 2007/Revised October 15, 2007/Accepted October 28, 2007/Online publication February 4, 2008)

**Refractoriness to carcinogen-induced increases in epithelial cell proliferation is a very important characteristic of parous mammary glands. We found that *N*-methyl-*N*-nitrosourea (MNU)-induced proliferative burst in the mammary ductal epithelium was blocked in parous glands but not in age-matched virgin (AMV) glands. The inhibition of the proliferative burst in MNU-treated parous mammary glands coincided with the upregulation of Mnt, a Myc-suppressor, and the formation of histone deacetylase 1/Mnt/Max complexes that unexpectedly contained c-Myc. These complexes formed on the promoters of Myc targets, such as ornithine decarboxylase, cyclin D2, and transforming growth factor β1 genes, in quiescent fibroblasts, and were disassembled in serum-stimulated cells. These results suggest that the complexes also function as transcription repressors of the growth-related Myc targets in MNU-treated parous mammary glands. Using the chemical mammary carcinogenesis model of human *c-Ha-ras* transgenic (Tg) rats, we confirmed that parity protected the mammary glands at the postinitiation phase of tumorigenesis. Although the incidence of 7,12-dimethylbenz[α]anthracene-induced palpable tumors was reduced from 61.5% in the AMV Tg rats to 28.5% in the parous animals, the incidence of early neoplastic lesions in the parous rats was the same as that in the AMV rats. Restriction fragment length polymorphism analysis detected mutations in the human *c-Ha-ras* gene in most of the normal-appearing parous Tg glands, as well as in the virgin glands. We propose that accelerated formation of HDAC1/c-Myc/Mnt/Max complexes in response to carcinogen exposure results in down-regulation of growth-related genes, leading to the refractoriness of parous mammary glands at the postinitiation phase of carcinogenesis. (*Cancer Sci* 2008; 99: 309–315)**

Strong epidemiological evidence indicates that women who experience a full-term pregnancy early in their lives have a significantly reduced risk of developing breast cancer.[1,2] In both rat and mouse models, full-term pregnancy confers resistance to chemical carcinogen-induced mammary tumorigenesis[3,4] and this effect can be mimicked by treatment with estrogen,[5] estrogen and progesterone,[4] or human chorionic gonadotropin.[6] However, the actual mechanism involved in parity protection or hormone-induced protection against breast cancer has not yet been clearly defined. The most widely accepted explanation for pregnancy protection against mammary cancer is that the pregnancy-induced differentiation of terminal end buds and terminal ducts reduces the number of target cells for carcinogenesis.[7] It has also been reported that parous rats have decreased levels of mammogenic hormones, and this decrease has been attributed to the decreased incidence of mammary cancers in these animals.[8,9] However, complete differentiation of the mammary gland does not appear to be an obligatory prerequisite for protection against mammary carcinogenesis.[4,10,11] We have shown that pregnancy following carcinogen exposure as well as pregnancy prior to carcinogen exposure reduces mammary carcinogenesis in rats.[12] This result indicates that pregnancy has the potential to affect the carcinogen-initiated cells that are static at the promotion phase, thus providing further support to the conclusion mentioned above.

The proto-oncogene *myc* has long been known to stimulate cellular proliferation. Aberrant expression of Myc in the mammary glands of transgenic mice results in the development of invasive mammary adenocarcinomas.[13,14] Myc proteins are basic helix–loop–helix leucine-zipper (bHLH-Zip) transcription factors whose function relies on heterodimerization with Max through their related bHLH-Zip domain.[15] The Myc–Max heterodimer binds to E-box DNA sequences (CAYGTG) and can activate transcription through a tethered complex of proteins that contains histone acetyltransferase and other activities that remodel chromatin.[16] Max also heterodimerizes with several other proteins that contain Myc-like bHLH-Zip domains, including the Mad family proteins Mxd 1–4, the Mad-related protein Mnt, and Mga.[17,18] These are all transcription repressors that can block Myc-dependent cell transformation.[19,20] The transcription repression activity of Mnt and Mxd 1–4 is dependent on the interaction with Sin 3A and Sin 3B co-repressors.[16] Sin 3A and Sin 3B interact with a number of different proteins, including histone deacetylase (HDAC)1 and HDAC2.[21,22] A current working model proposes that E-boxes are occupied by Mnt–Max in quiescent cells, whereas Mnt–Max complexes are displaced by Myc–Max complexes in growth-stimulated cells.[23,24] Furthermore, Mnt deletion provokes many responses triggered by Myc, even in cells lacking *c-myc*.[18,25] Therefore, Mnt has been proposed to be a tumor suppressor behaving as a master regulator of the Max network.[26,27] Strikingly, conditional inactivation of Mnt in mammary epithelium leads to elevation of cell proliferation and development of adenocarcinomas.[25,28]

In the present study, we found a close correlation between accelerated formation of novel HDAC1/c–Myc/Mnt/Max complexes and suppression of the proliferative burst in *N*-methyl-*N*-nitrosourea (MNU)-treated parous mammary glands. These quaternary complexes were assembled on the promoters of Myc-target genes in quiescent fibroblasts and were disassembled after proliferative stimulation of the cells. In addition, parity effectively protected the mammary glands from carcinogenesis mainly at the postinitiation phase.

[3]To whom correspondence should be addressed. E-mail: matsuoyo@takii.kmu.ac.jp

doi: 10.1111/j.1349-7006.2007.00689.x
© 2008 Japanese Cancer Association

## Materials and Methods

**Animals and treatment.** Nine-week-old female Lewis rats (Charles River Laboratories Japan, Kanagawa, Japan) were divided into two groups. Animals in the first group ($n = 25$) were mated and allowed to complete their pregnancy and nurse their litters (at least eight pups for each mother) for 21 days; the second group consisted of age-matched virgin (AMV) rats ($n = 25$). Each group was maintained for 4 additional weeks prior to receiving an i.p. injection of 50 mg/kg body weight of MNU (Wako Pure Chemical, Osaka, Japan) or vehicle only (1 mM HCl) at 19 weeks of age. Five animals in each group were killed before the injection and at 1, 3, 7, and 35 days after the injection. One side of the abdominal–inguinal mammary glands was removed, quick-frozen in liquid nitrogen, homogenized, and kept at –80°C until use. The other side of the glands was fixed overnight in 10% neutral-buffered formalin and embedded in paraffin.

In a separate experiment, female transgenic (Tg) rats with Sprague–Dawley background were used to assess the protective effect of pregnancy on mammary carcinogenesis. Briefly, the animals were separated into the AMV and parous groups as described above. The latter group of rats was mated at 7 weeks of age and allowed to complete their pregnancy and lactation. Each group then received an intragastric intubation of 50 mg/kg body weight of dimethylbenz(a)anthracene (DMBA; Tokyo Chemical Industries, Osaka, Japan) or the vehicle only (corn oil) at 15 weeks of age. The animals were maintained for 20 weeks then killed. DMBA instead of MNU was used as the mammary carcinogen as MNU causes malignancies of multiple organs in carcinogen-sensitive Tg rats, resulting in unexpected deaths of the animals during experiments. The tumor incidence was assessed by palpation during the period prior to euthanasia. 'Early neoplastic lesions' included atypical ductal hyperplasia and small adenocarcinomas identified by microscopic examination of the abdominal–inguinal mammary glands that did not have palpable tumors. All animal experiments were conducted according to the Guidelines for Animal Experimentation of Kansai Medical University (Osaka, Japan).

**Quantitation of cell proliferation in mammary ductal epithelium.** To analyze cell proliferation, the rats were injected, i.p., with 100 mg/kg body weight of bromodeoxyuridine (BrdU; Wako Pure Chemical) 1 h before they were killed. Tissue sections were deparaffinized and rehydrated according to standard protocols, incubated in 1 N HCl for 20 min, and in 0.01% actinase E (Kaken Pharmaceutical Co., Tokyo, Japan) in phosphate-buffered saline (PBS) for 5 min at 37°C, then blocked with 1% skim milk in PBS for 1 h. Mouse monoclonal anti-BrdU antibody (1:200 dilution) (Becton Dickinson, Franklin Lakes, NJ) was applied overnight at 4°C, and the immunocomplexes were visualized using a Vectastain ABC kit (Vector Laboratories, Burlingame, CA) according to the manufacturer's protocol. Labeling indices were calculated for >300 ductal epithelial cells.

**TdT-mediated dUTP-biotin nick-end labeling.** Apoptotic cells in the mammary ducts were detected by using a TdT-mediated dUTP-biotin nick-end labeling-based detection kit according to the manufacturer's protocol (Chemicon International, Temecula, CA). At least three microscopic fields viewed with a 40× objective were counted in each rat, representing a total of >1000 cells.

**Cell culture.** 3Y1 rat fibroblasts were maintained in Dulbecco's modified Eagle's medium containing 10% fetal calf serum. For serum starvation, 3Y1 cells were grown to subconfluency then rendered quiescent by incubation in Dulbecco's modified Eagle's medium containing 0.1% serum. In some experiments, after serum starvation for 3 days, the cells were incubated with 10% serum for 3 h.

**Reverse transcription–polymerase chain reaction (RT-PCR).** First-strand cDNA synthesis from total RNA and PCR amplifications using the following primers were carried out as described elsewhere:[29,30] *ODC* forward, 5′-ATGGGCAGCTTTACTAAGGAAGAG-3′, reverse, 5′-CTGAGCCGACAAACTGCTTTGGAAT-3′; *Ccnd2* forward, 5′-CCGCAACCTGCTGGAAGACC-3′, reverse, 5′-TCACAGGTCAACATCCCGCAC-3′; *Tgfb1* forward, 5′-AGACCATCGA CATGGAGCTG GTGAA-3′, reverse, 5′-CAAAAGACAG CCACTCAGGC GTATC-3′; *gapdh* forward, 5′-TTCAACGGCACAGTCAAGG-3′, reverse, 5′-CATGGACTGTGGTCATGAG-3′. The expression of *ODC* was expressed as the value of *ODC*/*gapdh* assessed by densitometric scans of agarose gels.

**Immunoprecipitation.** Extracts from the homogenized mammary glands (25 mg) and 3Y1 cells were prepared in immunoprecipitation buffer (50 mM Tris-HCl pH 7.5, 150 mM NaCl, 5 mM ethylenediaminetetraacetic acid (EDTA), 1% Triton X-100, 0.5% IGEPAL-CA630, 1 mM dithiothreitol, 1 mM $Na_3VO4$, 1 μM okadaic acid, 1 μM phenylmethylsulphonyl fluoride, and 10 μg/mL leupeptin). In the case of mammary glands, five individual lysates at each time point were combined and subjected to the following procedure. For preclearing, 1 mL of the extract was mixed with 50 μL of protein G magnetic bead suspension (New England Biolabs, Beverly, MA), rotated for 1 h at 4°C, and applied to a magnetic field for 5 min at 4°C. Extracts were then incubated with the indicated antibodies for 2 h at 4°C, and the antigen–antibody complexes were collected with the protein G beads for 1 h at 4°C. Protein complexes were washed twice with the low-salt chromatin immunoprecipitation (ChIP) wash buffer as described below and washed once with TE buffer (10 mM Tris-HCl, pH 8.0, 1 mM EDTA). Then proteins were separated by sodium dodecyl sulfate (SDS)–polyacrylamide gels.

**Immunoblot.** Western blot analysis was carried out as described previously.[31] The following antibodies were used: goat polyclonal anti-ODC antibody (sc-21515; 0.8 μg/mL); rabbit polyclonal anti-HDAC1 (sc-7872; 0.8 μg/mL); antic-Myc (sc-764; 0.8 μg/mL); anti-Mnt (sc-769; 0.8 μg/mL); anti-Mad1 (sc-222; 0.8 μg/mL); and anti-Max (sc-765; 0.8 μg/mL) antibodies, all from Santa Cruz Biotechnology (Santa Cruz, CA); and mouse monoclonal antiβ-actin antibody (1:500 dilution; Sigma, St. Louis, MO). The primary antibodies were detected using horseradish peroxidase-conjugated goat antirabbit (Cell Signaling Technology, Beverly, MA) and rabbit antigoat immunoglobulin (Ig)G antibodies (Invitrogen, Carlsbad, CA) and enhanced chemiluminescence plus Western blotting detection reagents (Amersham Biosciences, Piscataway, NJ).

**Restriction fragment length polymorphism (RFLP) analyses.** Three to five regions of ducts or neoplastic lesions from abdominal mammary glands were carefully scraped out of paraffin sections with scalpels, and DNA was extracted using Takara DEXPAT (Takara Biomedicals, Ohtsu, Japan). RFLP analyses of codon 12 of the human *c-Ha-ras* transgene were carried out as described previously.[32]

**ChIP assay.** Sub-confluent (~80%) cultures of randomly growing and 3-day serum-starved 3Y1 cells on ϕ10-cm dishes were cross-linked with 1% (w/v) formaldehyde in PBS at room temperature (20°C) for 10 min. The cross-linking reaction was stopped by adding glycine to a final concentration of 0.125 M. The cells were pelleted and lyzed in ChIP lysis buffer (50 mM Tris/HCl, pH 8.1, 10 mM EDTA, and 1% SDS) plus protease inhibitors (1 mM phenylmethylsulphonyl fluoride, 10 μg/mL aprotinin, and 10 μg/mL leupeptin). Lysates were sonicated until the DNA fragments were 600–1000 bp long then diluted 10-fold with immunoprecipitation dilution buffer (0.01% SDS, 1.1% Triton X-100, 1.2 mM EDTA, 16.7 mM Tris-HCl, pH 8.1, and 167 mM NaCl). Samples for total chromatin (input) were collected at this point to use as positive controls in the PCR. For preclearing, 300 mL of the diluted sample per antibody was mixed with 6 mg bovine serum albumin, 0.2 mg normal rabbit IgG, and 20 mL salmon sperm DNA/Protein G–agarose suspension (Upstate Biotechnology, Lake Placid, NY), rotated for 60 min at 4°C, and



doi: 10.1111/j.1349-7006.2007.00689.x
© 2008 Japanese Cancer Association

spun at 13 000*g* for 1 min at 4°C. The diluted samples (300 μL) were mixed with 1 μg each of normal rabbit IgG, anti-HDAC1 (sc-7872X), antic-Myc (sc-764X), anti-Mnt (sc-769X), or anti-MAX (sc-765X) antibody purchased from Santa Cruz Biotechnology and rotated overnight at 4°C. The samples were then mixed with 20 μL of salmon sperm DNA/Protein G–agarose suspension (Upstate Biotechnology) and rotated for 60 min at 4°C. Immune complexes were collected by centrifugation, washed with 1 mL each of low-salt wash buffer (20 mM Tris-HCl, pH 8.1, 150 mM NaCl, 2 mM EDTA, 0.1% SDS, 1% Triton X-100), high-salt wash buffer (20 mM Tris-HCl, pH 8.1, 500 mM NaCl, 2 mM EDTA, 0.1% SDS, 1% Triton X-100), LiCl buffer (10 mM Tris-HCl, pH 8.1, 250 mM LiCl, 1% IGEPAL-CA630, 1% deoxycholic acid), then with TE buffer (10 mM Tris-HCl, pH 8.0, 1 mM EDTA) twice. Immune complexes were eluted twice in 100 μL of elution buffer (100 mM $NaHCO_3$ and 1% SDS) at room temperature for 15 min. DNA–protein cross-links were reversed by incubation with 200 mM NaCl at 65°C for 4 h for all samples, including the total input sample. The DNA was incubated sequentially with 50 μg/mL of RNase A at 37°C for 30 min and 50 μg/mL of proteinase K at 55°C for 1 h then purified with the GenElute Mammalian Genomic DNA Purification Kit (Sigma) according to the manufacturer's instructions. PCR amplification of the intronic E-box-containing region in the rat *ODC* promoter was carried out with the following set of primers: forward, 5′-TGCGGCGGGCTCGACGAGGCGGCTGA-3′; reverse, 5′-TCCCC-TGCCGGCGACCGCAGTC-3′.

**Statistics.** All statistical evaluations were carried out with multiple comparison by Sheffe's *F*-test in Statcel 2 for Excel (OMS Publishing Inc, Tokorozawa, Japan).

## Results

**Proliferative burst triggered by MNU exposure was blocked in parous mammary glands.** As a differential regulation of cell proliferation and cell death could explain the difference in sensitivity to carcinogenesis for nulliparous and parous mammary glands, we analyzed cell proliferation in each of the glands after MNU challenge (Fig. 1). At 19 weeks of age, before the carcinogen inoculation, the proliferation was low in the AMV (2.4%) as well as parous (2.3%) mammary glands. The proliferation remained low in both AMV and parous glands 3 days after the challenge (2.3% and 1.8% for virgin and parous, respectively). However, 7 days after MNU inoculation, the BrdU labeling index in the parous glands (1.3%) was significantly lower than that in the AMV glands (3.6%, $P < 0.05$). At day 35 after the treatment, the proliferation was lower in both types of glands, but was still relatively higher in the virgin (1.7%) glands than in the parous glands (1.3%) (Fig. 1). There was no significant difference in apoptotic cell deaths between the virgin and parous ductal epithelia (virgin, 1.07 ± 0.46%, parous, 0.93 ± 0.09%) at 7 days after MNU injection.

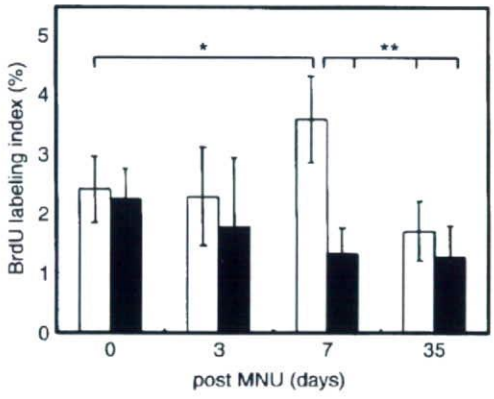


**Fig. 1.** Comparison of cell proliferation between age-matched virgin (AMV; open columns) and parous (solid columns) rat mammary glands after *N*-methyl-*N*-nitrosourea (MNU) inoculation. Bromodeoxyuridine-labeling indices in the mammary ductal epithelium of AMV and parous rats at 0, 3, 7, and 35 days after MNU injection. Each value represents mean ± SD calculated from five glands at each time point. Differences between groups were tested for statistical significance by using Sheffe's *F*-test. $*P < 0.05$; $**P < 0.01$.

**Upregulation of Myc-suppressor Mnt and accelerated formation of novel HDAC1/c-Myc/Mn/Maxt complexes in MNU-treated parous mammary glands.** We then examined the mechanism underlying parity-induced suppression of proliferative burst after carcinogen treatment. As an initial approach, the levels of c-Myc, Mnt, Mad1, and Max were compared between virgin and parous mammary glands at 0 and 7 days after MNU injection, because each of these proteins forms functionally different protein complexes with Max to regulate the expression of the Myc-target genes. The most significant difference in the two types of glands was observed for the level of Mnt at 7 days after MNU exposure. Mnt was significantly higher in the parous glands compared to the AMV glands. Actually, Mnt tended to increase in the parous glands, whereas Mnt significantly decreased in the AMV glands at this time point after the exposure (Fig. 2). It is noteworthy that the level of Max at 7 days after the exposure in the parous but not in the AMV glands was significantly ($P < 0.05$) higher than the levels before MNU exposure in the respective glands. There were no significant differences in any of these protein levels in the AMV and parous glands before the treatment, and the levels of c-Myc and Mad1 were stable (Fig. 2).

Immunoprecipitation experiments were carried out to determine if more HDAC1 was recruited into Mnt/Max transcription-repressor complexes in the MNU-treated parous mammary glands because of the increased level of Mnt. Indeed, higher amounts of HDAC1 co-immunoprecipitated with Mnt/Max complexes from the lysate of parous glands as compared to that of virgin glands after MNU treatment (Fig. 3a). Surprisingly, a large amount of c-Myc was associated with the HDAC1/Mnt/Max complexes in the MNU-treated parous glands (Fig. 3a). Other experiments using anti-HDAC1, antic-Myc, and anti-Max antibodies confirmed that c-Myc was trapped in the ternary complexes in the MNU-exposed parous glands (Fig. 3b and data not shown). HDAC1/c-Myc/Mnt/Max complexes were also detected in the virgin and parous glands before MNU exposure. However, c-Myc appeared to be released from the quaternary complexes in the virgin glands after the treatment (Fig. 3). It is also noteworthy that a higher amount of Mad1 was associated with Mnt–Max complexes in the parous glands compared to the virgin glands before MNU challenge (Fig. 3a). Thus, it is possible that the HDAC1/c-Myc/Mnt/Max complexes preferentially form in place of the HDAC1/Mad1/Mnt/Max complexes after the carcinogenic stimuli in the parous glands.

**HDAC1/c-Myc/Mnt/Max complexes are potential transcription repressors.** We then examined whether the formation of HDAC1/c-Myc/Mnt/Max complexes has a causal relationship to the downregulation of cell proliferation and gene expression. When 3Y1 rat fibroblasts were starved for serum, protein levels of c-Myc and Mnt in the nucleus gradually increased (data not shown), whereas expression levels of the *ODC*, *Ccnd2*, and *Tgfb1* genes, which are established targets of c-Myc, were reciprocally reduced (Fig. 4a). In the quiescent cells, c-Myc was trapped in anti-Mnt immunoprecipitates that also contained HDAC1, and these complexes were disassembled by the growth stimuli (Fig. 4b). ChIP assays clearly indicated the assembly and disassembly of the quaternary complexes on the promoter (presumably on the E-boxes) of *ODC* in the quiescent and proliferating cells, respectively (Fig. 4c). The same results were obtained for the promoters of *Ccnd2* and *Tgfb1* (data not shown). Therefore, we


© 2008 Japanese Cancer Association

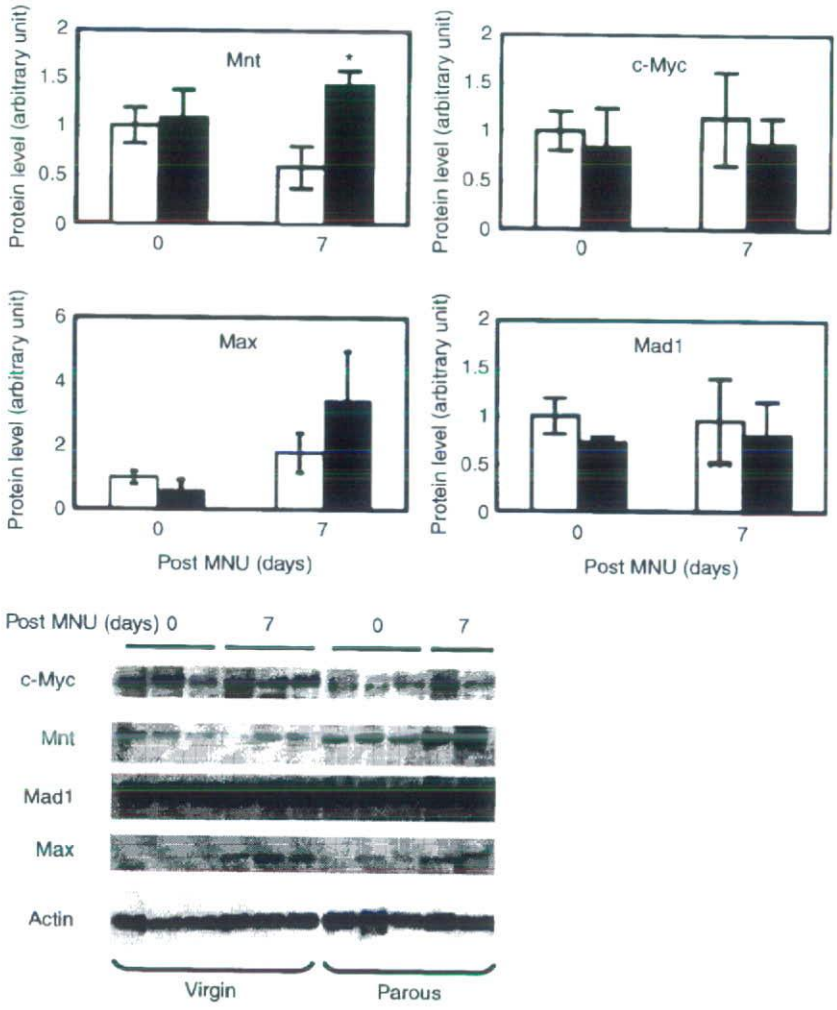


**Fig. 2.** Immunoblot analyses of levels of the c-Myc regulators in age-matched virgin (AMV; open columns) and parous (solid columns) rat mammary glands after *N*-methyl-*N*-nitrosourea exposure. Changes in the protein levels of the E-box-interacting proteins were monitored with immunoblots at 0 and 7 days after the carcinogen inoculation. Densitometric quantification data ($n = 5$ at each time point) were obtained from three independent blots. The mean value of the AMV glands at day 0 is expressed as 1, and each value represents mean ± SD. $^*P < 0.05$ *versus* AMV at the indicated time point. The blots are representative of three independent experiments. Actin was used as a loading control.

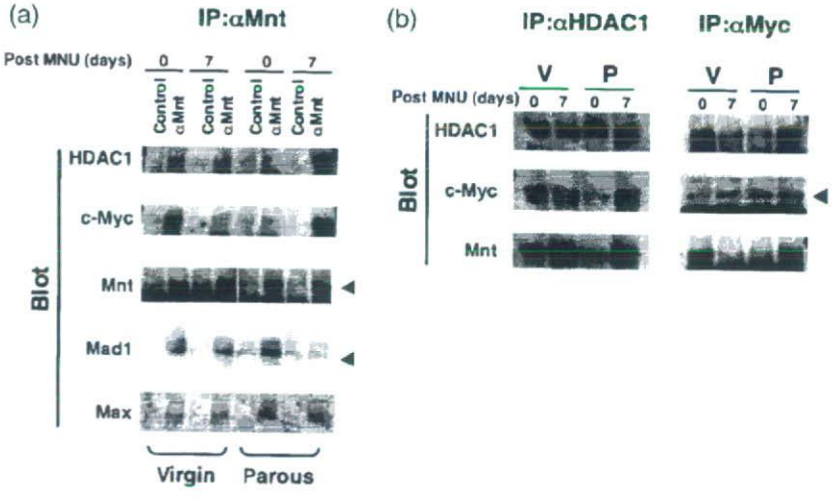


**Fig. 3.** Induction of HDAC1/c-Myc/Mnt/Max complex formation in *N*-methyl-*N*-nitrosourea (MNU)-treated parous rat mammary glands. (a) Western blot data from immunoprecipitation with anti-Mnt antibody from each combined lysate of age-matched virgin (V) and parous (P) mammary glands ($n = 5$ each) at 0 and 7 days after MNU treatment. Normal rabbit immunoglobulin G was used as the control. (b) Immunoblot data from immunoprecipitations with anti-HDAC1 (αHDAC1) and anti-c-Myc (αMyc) antibodies from the corresponding samples in panel (a). Note the induction of HDAC1/c-Myc/Mnt association in the parous sample after MNU treatment. The immunoprecipitations were carried out simultaneously in three independent experiments. Arrows indicate the corresponding protein bands. IP, immunoprecipitation.

concluded that the formation of novel HDAC1/c-Myc/Mnt/Max quaternary complexes contributes to downregulation of the Myc-target genes and cell proliferation in parous mammary glands after carcinogen exposure.

**Parity protects mammary carcinogenesis at the postinitiation phase.** The carcinogenesis model of human *c-Ha-ras* Tg rats was used to directly test our hypothesis that there is a major postinitiation effect of parity in protection from mammary tumorigenesis.



doi: 10.1111/j.1349-7006.2007.00689.x
© 2008 Japanese Cancer Association

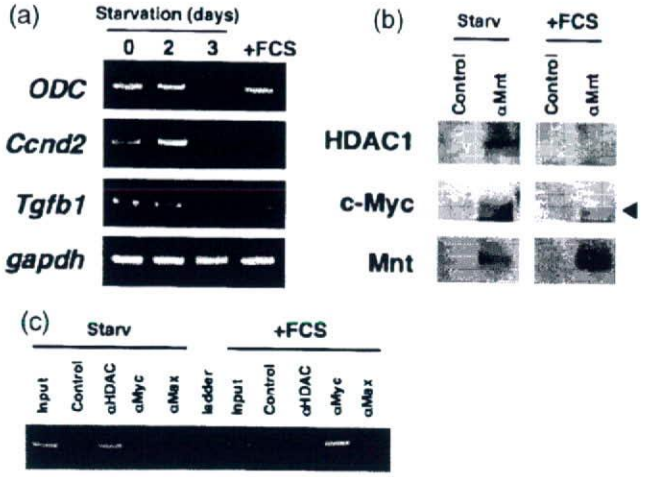


**Fig. 4.** Assembly and disassembly of HDAC1/c-Myc/Mnt/Max complexes on the promoter of Myc-target gene in fibroblasts. (a) Reverse transcription–polymerase chain reaction analysis of mRNA expression of Myc-target genes during serum starvation. The suppression of target gene expressions was relieved 3 h after restimulation by serum of the quiescent fibroblasts (+FCS). (b) Western blot data from immunoprecipitation with anti-Mnt antibody from the quiescent (Starv) and serum-stimulated (+FCS) fibroblast lysates. Normal rabbit immunoglobulin (Ig)G was used as the control. (c) Chromatin immunoprecipitation assays of the quiescent (Starv) and serum-stimulated (+FCS) fibroblasts were carried out using antibodies against HDAC1, c-Myc, or Max. Normal rabbit IgG was used as the control.

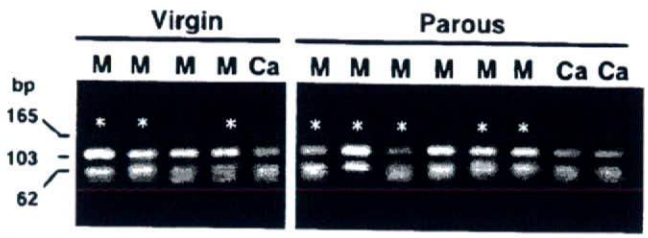


**Fig. 5.** Mutations in the human *c-Ha-ras* genes in the mammary glands of transgenic (Tg) age-matched virgin (AMV) and parous rats after dimethylbenz(a)anthracene treatment. Representative restriction fragment length polymorphism analysis data for codon 12 of the human *c-Ha-ras* gene. DNA samples were collected from several regions of normal mammary ducts in AMV and parous rats. *Presence of 165 bp bands corresponding to the mutant human *c-Ha-ras*. Ca, DNA from three individual microscopic carcinomas in virgin and parous Tg rats; M, DNA from mammary ductal epithelium with normal morphology.

Mammary tumors became palpable in 1 of 13 AMV Tg rats at 6 weeks after DMBA inoculation, and the tumor incidence gradually increased to 61.5% at 20 weeks. In contrast, the first tumor became palpable in a parous Tg rat at 12 weeks, and only 28.5% (4/14) of the animals developed lesions by 20 weeks (Table 1). Although there was not a significant difference in the mean weight of the mammary tumors in the two groups at the time of autopsy, significantly fewer tumors per animal were observed in the parous rats than in the AMV animals (Table 1). Thus, parity was protective against carcinogen-induced tumorigenesis even in this highly tumorigenic rat strain. However, microscopic surveys of mammary glands that lacked palpable tumors from all rats revealed that the incidence of early neoplastic lesions (atypical hyperplasia and small adenocarcinomas) did not differ between the AMV (53.8%) and parous (64.3%) groups at 20 weeks.

As the mutation rate of the human *c-Ha-ras* transgene is markedly higher than that of the endogenous rat gene, the transgene was used as a probe to monitor ras mutations, thought to occur during the initiation step of carcinogenesis. RFLP analysis detected mutations in codon 12 of the human Ha-ras transgene in most of the normal epithelial samples, regardless of their parous status (Fig. 5). Therefore, the initiation steps occurred with equal frequency in the virgin and parous mammary glands of Tg rats. In conclusion, parity effectively protects the mammary glands from cancer development by a reduction in cell proliferation mediated by the formation of HDAC1/c-Myc/Mnt/Max complexes even at the promotion and/or progression phases of carcinogenesis.

## Discussion

An early full-term pregnancy induces a refractory state of the mammary gland against carcinogenesis in both humans[1,2] and rodents.[3,12] Despite extensive efforts to reveal the mechanisms of parity-induced protection against mammary cancer, the cellular and molecular mechanisms are still largely unresolved. The most widely accepted explanation for pregnancy protection against mammary cancer is that the protective effect is attributable to the pregnancy-induced differentiation of the target structures, terminal end buds and terminal ducts.[33] A corollary to this hypothesis is that differences in susceptibility to carcinogen-induced tumorigenesis between parous and nulliparous glands could be explained by the differences in proliferation indices, alterations of the properties associated with carcinogen uptake, binding, and metabolism, and an enhanced capacity for DNA repair.[7] However, studies in which differentiation of the mammary glands was achieved by hormonal stimulation have indicated that the protective effect is independent of the level of differentiation.[4,5,10,11] Furthermore, other studies have shown no consistent differences in cellular kinetics between parous and nulliparous animals.[10]

Estrogen alone or estrogen plus progesterone treatment can induce protection from mammary carcinogenesis in rats and mice.[5,34] Using this model, Sivaraman *et al.*[35] showed that an important molecular alteration that occurs in the hormone-treated gland is the induction, sustained expression, activation, and nuclear sequestration of p53 tumor suppressor protein. This change is persistent and present at the time of carcinogen treatment. Furthermore, the absence of the p53 gene abrogates

**Table 1. Incidences and numbers of gross mammary tumors in transgenic rats at 20 weeks after *N*-methyl-*N*-nitrosourea injection**

| | No. of rats | Atypical hyperplasia | | Adenocarcinoma | | Total | | Weight of tumors/rat (g) (mean ± SD) |
|---|---|---|---|---|---|---|---|---|
| | | Incidence (%) | No./rat (mean ± SD) | Incidence (%) | No./rat (mean ± SD) | Incidence (%) | No./rat (mean ± SD) | |
| Virgin | 13 | 1 (7.7) | 0.08 ± 0.277 | 8 (61.5) | 1.92 ± 2.99 | 8 (61.5) | 2.00 ± 2.97 | 5.37 ± 14.04 |
| Parous | 14 | 1 (7.7) | 0.07 ± 0.267 | 4 (28.5) | 0.43 ± 0.85* | 4 (28.5) | 0.50 ± 0.94* | 2.20 ± 7.94 |

*$P < 0.05$, as compared to Virgin.


© 2008 Japanese Cancer Association

the protective effect of hormones against carcinogen-induced mammary carcinogenesis in mice.[34] Therefore, the authors developed a cell-fate hypothesis that proposes that at a critical period in adolescence the hormonal milieu of pregnancy affects the developmental fate of a subset of mammary epithelial cells. This hypothesis is attractive and might explain parity-induced protection against mammary cancer at the initiation phase of carcinogenesis when DNA damage is thought to occur.

However, several laboratories have reported that the short-term inoculation of ovarian steroids (estrogens and progesterone) or human chorionic gonadotropins not only before but also after carcinogen treatment decreases the incidence of mammary carcinomas in rodents.[4,11,36] Moreover, we have shown that pregnancy following the carcinogen exposure also reduces mammary carcinogenesis in rats.[12] Human *c-Ha-ras* proto-oncogene Tg rats have an increased susceptibility to chemical carcinogens that target the mammary gland.[37,38] All of the rats developed preneoplastic mammary lesions within 20 days of the injection of MNU[39] and mammary carcinomas appeared within 8 weeks of treatment with a variety of chemical carcinogens.[29,40] Interestingly, activating mutations in the human transgene are readily detectable in preneoplastic lesions that developed after carcinogen treatment or spontaneously.[29] Therefore, mammary carcinogenesis in Tg rats is an excellent model to study multistep development of cancers. In the present study, we found that parity effectively protected the Tg mammary glands as well as the wild-type glands from carcinogenesis preferentially at the postinitiation phase (Table 1 and Fig. 5). Therefore, both pregnancy and the hormones might have potential to protect mammary glands from carcinogenesis at the postinitiation phase.

The most striking finding in the present study was the discovery of HDAC1/c-Myc/Mnt/Max complexes in the MNU-treated parous mammary glands and the quiescent rat fibroblasts. We have also found assembly and disassembly of HDAC1/c-Myc/Mnt/Max complexes in the quiescent and growth-stimulated fibroblasts, respectively (Fig. 4). Thus, based on our findings, c-Myc/Mnt/Max interactions probably are more complex in some types of cells as compared to the current model, in which Mnt–Max and Myc–Max complexes are mutually exclusively formed depending on the growth states of cells.[23,24] Induction of *c-myc* mRNA and protein expression in quiescent fibroblasts and transformed epithelial cells has previously been shown, although the precise role of c-Myc in these cells is still unclear.[41,42] One laboratory has suggested a role for c-Myc 1, the non-AUG-initiated form of the c-Myc protein, in growth inhibition of cells.[43] Interestingly, in the parous mammary glands after MNU treatment, we found the accelerated formation of HDAC1/c-Myc/Mnt/Max complexes as seen in the fibroblasts. DNA damage generated by carcinogens such as MNU and DMBA induces *ODC* expression, replicative DNA synthesis, and cell proliferation in different types of cells including mammary epithelium and fibroblasts under certain conditions ([44,45] and Matsuoka *et al.* this study and unpublished data, 2007). Therefore, it is reasonable to propose that HDAC1/c-Myc/Mnt/Max quaternary complexes function as transcription repressors of growth-related genes such as *ODC* and *Ccnd2* at the promotion phase of preneoplastic epithelial cells in parous mammary glands. Indeed, we have previously shown that the parous glands show signs of inhibition of upregulation of growth-related genes including *ODC*, *Stmn1*, *Cdc2a*, *Igf2*, and *Msln* at 21 days after MNU treatment.[46]

In summary, our results indicate that full-term pregnancy leads to the accelerated formation of HDAC1/c-Myc/Mnt/Max complexes in parous mammary glands when they are exposed to DNA-damaging agents. The quaternary complexes might function as transcription repressors to directly and/or indirectly downregulate growth-related genes; this downregulation leads to refractoriness of the parous glands, probably at the promotion phase of carcinogenesis. The differentiation theory proposed by Russo *et al.*[33] and the cell-fate theory proposed by Medina and Kittrell[34] to explain parity-induced protection mainly apply to the initiation phase of mammary carcinogenesis. Hence, we speculate that the protection provided by parity might operate with different molecular mechanisms at both the initiation and promotion phases. Because it is impossible to determine when mammary epithelial cells are initiated for tumorigenesis in humans, protection at the initiation phase of breast cancer by practical means such as hormone treatments might be incomplete. Rajkumar *et al.*[5] recently showed that short-term exposure to pregnancy levels of estrogen after carcinogen inoculation effectively induces refractoriness to mammary carcinogenesis in rats. Therefore, we believe that protection at the promotion phase is more practical than protection at the initiation phase. We are currently working to identify all constituents of the HDAC1/c-Myc/Mnt/Max complexes in mammary glands as well as in fibroblasts. This information will provide deeper insights into the underlying mechanisms of parity-induced and hormone-induced protection against mammary cancer.

## Acknowledgments

We are grateful to Dr Tetsuya Hamaguchi, Mie University School of Medicine, and Ms. Takako Akamatsu for their technical support, and Dr Jumpei Enami, Zenyaku Kogyo Co., for his critical reading of the manuscript. This work was supported in part by a Grant-in-Aid for Scientific Research on Priority Areas (KAKENHI) from the Ministry of Education, Culture, Sports, Science and Technology of Japan, a Grant-in-Aid for the Second-term Comprehensive 10-Year Strategy for Cancer Control, a Grant-in-Aid for Cancer Research, a Health and Labor Science Research Grant for Research on Risk of Chemical Substances from the Ministry of Health, Labour and Welfare of Japan, and by the Nakayama Foundation for Human Science.

## References

1 Kelsey JL, Gammon MD. The epidemiology of breast cancer. *CA Cancer J Clin* 1991; 41: 146–65.
2 Rosner B, Colditz GA, Willett WC. Reproductive risk factors in a prospective study of breast cancer: the Nurses' Health Study. *Am J Epidemiol* 1994; **139**: 819–35.
3 Medina D, Smith GH. Chemical carcinogen-induced tumorigenesis in parous, involuted mouse mammary glands. *J Natl Cancer Inst* 1999; **91**: 967–9.
4 Guzman RC, Yang J, Rajkumar L, Thordarson G, Chen X, Nandi S. Hormonal prevention of breast cancer: mimicking the protective effect of pregnancy. *Proc Natl Acad Sci USA* 1999; **96**: 2520–5.
5 Rajkumar L, Guzman RC, Yang J, Thordarson G, Talamantes F, Nandi S. Short-term exposure to pregnancy levels of estrogen prevents mammary carcinogenesis. *Proc Natl Acad Sci USA* 2001; **98**: 11 755–9.
6 Grubbs CJ, Juliana MM, Whitaker LM. Short-term hormone treatment as a chemopreventive method against mammary cancer initiation in rats. *Anticancer Res* 1988; **8**: 113–17.
7 Russo IH, Russo J. Mammary gland neoplasia in long-term rodent studies. *Environ Health Perspect* 1996; **104**: 938–67.
8 Thordarson G, Jin E, Guzman RC, Swanson SM, Nandi S, Talamantes F. Refractoriness to mammary tumorigenesis in parous rats: is it caused by persistent changes in the hormonal environment or permanent biochemical alterations in the mammary epithelia? *Carcinogenesis* 1995; **16**: 2847–53.
9 Thordarson G, Van Horn K, Guzman RC, Nandi S, Talamantes F. Parous rats regain high susceptibility to chemically induced mammary cancer after treatment with various mammotropic hormones. *Carcinogenesis* 2001; **22**: 1027–33.
10 Sivaraman L, Stephens LC, Markaverich BM *et al.* Hormone-induced refractoriness to mammary carcinogenesis in Wistar–Furth rats. *Carcinogenesis* 1998; **19**: 1573–81.
11 Medina D, Peterson LE, Moraes R, Gay J. Short-term exposure to estrogen and progesterone induces partial protection against *N*-nitroso-*N*-methylurea-induced mammary tumorigenesis in Wistar–Furth rats. *Cancer Lett* 2001; **169**: 1–6.
12 Yang J, Yoshizawa K, Nandi S, Tsubura A. Protective effects of pregnancy and lactation against *N*-methyl-*N*-nitrosourea-induced mammary carcinomas in female Lewis rats. *Carcinogenesis* 1999; **20**: 623–8.



doi: 10.1111/j.1349-7006.2007.00689.x
© 2008 Japanese Cancer Association

13 Schoenenberger CA, Andres AC, Groner B, van der Valk M, LeMeur M, Gerlinger P. Targeted *c-myc* gene expression in mammary glands of transgenic mice induces mammary tumours with constitutive milk protein gene transcription. *EMBO J* 1988; 7: 169–75.
14 D'Cruz CM, Gunther EJ, Boxer RB *et al.* c-MYC induces mammary tumorigenesis by means of a preferred pathway involving spontaneous Kras2 mutations. *Nat Med* 2001; **7**: 235–9.
15 Eisenman RN. Deconstructing *myc*. *Genes Dev* 2001; **15**: 2023–30.
16 Hurlin PJ, Queva C, Eisenman RN. Mnt, a novel Max-interacting protein and Myc antagonist. *Curr Top Microbiol Immunol* 1997; **224**: 115–21.
17 Grandori C, Cowley SM, James LP, Eisenman RN. The Myc/Max/Mad network and the transcriptional control of cell behavior. *Annu Rev Cell Dev Biol* 2000; **16**: 653–99.
18 Zhou ZQ, Hurlin PJ. The interplay between Mad and Myc in proliferation and differentiation. *Trends Cell Biol* 2001; **11**: S10–14.
19 Ayer DE, Kretzner L, Eisenman RN. Mad: a heterodimeric partner for Max that antagonizes Myc transcriptional activity. *Cell* 1993; **72**: 211–22.
20 Hurlin PJ, Queva C, Koskinen PJ *et al.* Mad3 and Mad4: novel Max-interacting transcriptional repressors that suppress *c-myc* dependent transformation and are expressed during neural and epidermal differentiation. *EMBO J* 1995; **14**: 5646–59.
21 Ayer DE. Histone deacetylases: transcriptional repression with SINers and NuRDs. *Trends Cell Biol* 1999; **9**: 193–8.
22 Hurlin PJ, Huang J. The MAX-interacting transcription factor network. *Semin Cancer Biol* 2006; **16**: 265–74.
23 Bello-Fernandez C, Packham G, Cleveland JL. The ornithine decarboxylase gene is a transcriptional target of c-Myc. *Proc Natl Acad Sci USA* 1993; **90**: 7804–8.
24 Nilsson JA, Maclean KH, Keller UB, Pendeville H, Baudino TA, Cleveland JL. Mnt loss triggers Myc transcription targets, proliferation, apoptosis, and transformation. *Mol Cell Biol* 2004; **24**: 1560–9.
25 Hurlin PJ, Zhou ZQ, Toyo-oka K *et al.* Deletion of Mnt leads to disrupted cell cycle control and tumorigenesis. *EMBO J* 2003; **22**: 4584–96.
26 Hurlin PJ, Zhou ZQ, Toyo-Oka K *et al.* Evidence of *mnt–myc* antagonism revealed by *mnt* gene deletion. *Cell Cycle* 2004; **3**: 97–9.
27 Nilsson JA, Cleveland JL. Mnt: master regulator of the Max network. *Cell Cycle* 2004; **3**: 588–90.
28 Toyo-oka K, Bowen TJ, Hirotsune S *et al.* Mnt-deficient mammary glands exhibit impaired involution and tumors with characteristics of *myc* overexpression. *Cancer Res* 2006; **66**: 5565–73.
29 Hamaguchi T, Matsuoka Y, Kawaguchi H *et al.* Terminal endbuds and acini as the respective major targets for chemical and sporadic carcinogenesis in the mammary glands of human *c-Ha-ras* protooncogene transgenic rats. *Breast Cancer Res Treat* 2004; **83**: 43–56.
30 Fukamachi K, Matsuoka Y, Kitanaka C, Kuchino Y, Tsuda H. Rat neuronal leucine-rich repeat protein-3: cloning and regulation of the gene expression. *Biochem Biophys Res Comm* 2001; **287**: 257–63.
31 Fukamachi K, Matsuoka Y, Ohno H, Hamaguchi T, Tsuda H. Neuronal leucine-rich repeat protein-3 amplifies MAPK activation by epidermal growth factor through a carboxyl-terminal region containing endocytosis motifs. *J Biol Chem* 2002; **277**: 43 549–52.
32 Hamaguchi T, Matsuoka Y, Bechberger J *et al.* Establishment of an apoptosis-sensitive rat mammary carcinoma cell line with a mutation in the DNA-binding region of p53. *Cancer Lett* 2006; **232**: 279–88.
33 Russo J, Hu YF, Silva ID, Russo IH. Cancer risk related to mammary gland structure and development. *Microsc Res Tech* 2001; **52**: 204–23.
34 Medina D, Kittrell FS. p53 function is required for hormone-mediated protection of mouse mammary tumorigenesis. *Cancer Res* 2003; **63**: 6140–3.
35 Sivaraman L, Conneely OM, Medina D, O'Malley BW. p53 is a potential mediator of pregnancy and hormone-induced resistance to mammary carcinogenesis. *Proc Natl Acad Sci USA*, 2001; **98**: 12 379–84.
36 Swanson SM, Whitaker LM, Stockard CR *et al.* Hormone levels and mammary epithelial cell proliferation in rats treated with a regimen of estradiol and progesterone that mimics the preventive effect of pregnancy against mammary cancer. *Anticancer Res* 1997; **17**: 4639–45.
37 Asamoto M, Ochiya T, Toriyama-Baba H *et al.* Transgenic rats carrying human *c-Ha-ras* proto-oncogenes are highly susceptible to *N*-methyl-*N*-nitrosourea mammary carcinogenesis. *Carcinogenesis* 2000; **21**: 243–9.
38 Ota T, Asamoto M, Toriyama-Baba H *et al.* Transgenic rats carrying copies of the human *c-Ha-ras* proto-oncogene exhibit enhanced susceptibility to *N*-butyl-*N*-(4-hydroxybutyl) nitrosamine bladder carcinogenesis. *Carcinogenesis* 2000; **21**: 1391–6.
39 Matsuoka Y, Fukamachi K, Hamaguchi T *et al.* Rapid emergence of mammary preneoplastic and malignant lesions in human *c-Ha-ras* proto-oncogene transgenic rats: possible application for screening of chemopreventive agents. *Toxicol Pathol* 2003; **31**: 632–7.
40 Han BS, Fukamachi K, Takasuka N *et al.* Inhibitory effects of 17beta-estradiol and 4-n-octylphenol on 7,12-dimethylbenz[a]anthracene-induced mammary tumor development in human *c-Ha-ras* proto-oncogene transgenic rats. *Carcinogenesis* 2002; **23**: 1209–15.
41 Hann SR, Sloan-Brown K, Spotts GD. Translational activation of the non-AUG-initiated c-myc 1 protein at high cell densities due to methionine deprivation. *Genes Dev* 1992; **6**: 1229–40.
42 Martel C, Lallemand D, Cremisi C. Specific c-myc and max regulation in epithelial cells. *Oncogene* 1995; **10**: 2195–205.
43 Hann SR, Dixit M, Sears RC, Sealy L. The alternatively initiated c-Myc proteins differentially regulate transcription through a noncanonical DNA-binding site. *Genes Dev* 1994; **8**: 2441–52.
44 Fedrowitz M, Kamino K, Loscher W. Significant differences in the effects of magnetic field exposure on 7,12-dimethylbenz (a) anthracene-induced mammary carcinogenesis in two substrains of Sprague–Dawley rats. *Cancer Res* 2004; **64**: 243–51.
45 Cohn SM, Krawisz BR, Dresler SL, Lieberman MW. Induction of replicative DNA synthesis in quiescent human fibroblasts by DNA damaging agents. *Proc Natl Acad Sci USA* 1984; **81**: 4828–32.
46 Uehara N, Unami A, Kiyozuka Y, Shikata N, Oishi Y, Tsubura A. Parous mammary glands exhibit distinct alterations in gene expression and proliferation responsiveness to carcinogenic stimuli in Lewis rats. *Oncol Rep* 2006; **15**: 903–11.


© 2008 Japanese Cancer Association

# Comprehensive screening for antigens overexpressed on carcinomas via isolation of human mAbs that may be therapeutic

Gene Kurosawa[a], Yasushi Akahori[a], Miwa Morita[a], Mariko Sumitomo[b], Noriko Sato[c], Chiho Muramatsu[b], Keiko Eguchi[b], Kazuki Matsuda[b], Akihiko Takasaki[d], Miho Tanaka[a], Yoshitaka Iba[a], Susumu Hamada-Tsutsumi[a], Yoshinori Ukai[e], Mamoru Shiraishi[e], Kazuhiro Suzuki[e], Maiko Kurosawa[a], Sally Fujiyama[f], Nobuhiro Takahashi[f], Ryoichi Kato[g], Yoshikazu Mizoguchi[h], Mikihiro Shamoto[i], Hiroyuki Tsuda[j], Mototaka Sugiura[k], Yoshinobu Hattori[l], Shuichi Miyakawa[l], Ryoichi Shiroki[c], Kiyotaka Hoshinaga[c], Nobuhiro Hayashi[d], Atsushi Sugioka[l], and Yoshikazu Kurosawa[a,m]

[a]Division of Antibody Project and [d]Department of Biomedical Polymer Science, Institute for Comprehensive Medical Science, [b]21st Century Center of Excellence Research Center, Departments of [c]Urology, [g]Radiology, [h]Pathology, [k]Internal Medicine, and Surgery, School of Medicine, Fujita Health University, Toyoake, Aichi 470-1192, Japan; [e]Institute for Antibodies, Ltd., Toyoake, Aichi 470-1192, Japan; [f]Department of Biotechnology, United Graduate School of Agriculture, Tokyo University of Agriculture and Technology, Saiwai-cho, Fuchu-shi, Tokyo 183 8509, Japan; [i]Division of Clinical Laboratory, Yachiyo Hospital, Anjo, Aichi 446-8510, Japan; and [j]Department of Toxicology, Graduate School of Medical Sciences, Nagoya City University, Kawazumi, Mizuho, Nagoya 467-8601, Japan

Edited by Frederick W. Alt, Harvard Medical School, Boston, MA, and approved March 14, 2008 (received for review December 29, 2007)

**Although several murine mAbs that have been humanized became useful therapeutic agents against a few malignancies, therapeutic Abs are not yet available for the majority of the human cancers because of our lack of knowledge of which antigens (Ags) can become useful targets. In the present study we established a procedure for comprehensive identification of such Ags through the extensive isolation of human mAbs that may become therapeutic. Using the phage-display Ab library we isolated a large number of human mAbs that bind to the surface of tumor cells. They were individually screened by immunostaining, and clones that preferentially and strongly stained the malignant cells were chosen. The Ags recognized by those clones were isolated by immunoprecipitation and identified by MS. We isolated 2,114 mAbs with unique sequences and identified 21 distinct Ags highly expressed on several carcinomas. Of those 2,114 mAbs 356 bound specifically to one of the 21 Ags. After preparing complete $IgG_1$ Abs the *in vitro* assay for Ab-dependent cell-mediated cytotoxicity (ADCC) and the *in vivo* assay in cancer-bearing athymic mice were performed to examine antitumor activity. The mAbs converted to $IgG_1$ revealed effective ADCC as well as antitumor activity *in vivo*. Because half of the 21 Ags showed distinct tumor-specific expression pattern and the mAbs isolated showed various characteristics with strong affinity to the Ag, it is likely that some of the Ags detected will become useful targets for the corresponding carcinoma therapy and that several mAbs will become therapeutic agents.**

phage Ab library | therapeutic Ab | tumor-associated antigen

Since the discovery of a method to produce mAbs numerous scientists have been trying to identify and produce mAbs that could be used for immunotherapy against various malignancies. The success for example of alemtuzumab against CD52, trastuzumab against HER2, and rituximab against CD20 for treatment of chronic lymphocytic leukemia, breast cancer, and non-Hodgkins lymphoma, respectively (1–3), suggests that mAbs are likely to become very important therapeutic agents also against a wider range of cancers. However, for the majority of the human cancers useful therapeutic Abs are not yet available because of our lack of knowledge of which antigens (Ags) are likely to become useful targets (4). Therefore, several groups of investigators have been trying to identify other potential Ags as targets for immunotherapy using microarray technology (5, 6). Although many differences in transcripts have been revealed between malignant cells and the normal counterpart cells, it will take more time and laborious work to examine which Ags could be targets and to prepare therapeutic Abs against them. Furthermore, the presence of a large amount of transcripts does not always indicate expression of a large amount of the proteins.

Our experimental approach was designed in the opposite way to the strategy with the microarray technology mentioned above and was based on the phage-display technology (7). First we isolated a large number of mAbs that bind to the surface of cancer cells using a huge phage Ab library and many kinds of cancer-derived cell lines. Then using fresh tumor tissues we selected clones that gave significant staining of malignant cells but were negative or very weakly positive on the normal cells in the histological sections. At the third step the Ags recognized by the respective clones were isolated by immunoprecipitation and identified by MS analysis. Finally mAbs were converted to complete human $IgG_1$ and the antitumor activity was examined. Thus, the procedure adopted in our study enabled us to succeed in comprehensive identification of tumor-associated Ags (TAAs) and simultaneous isolation of mAbs against them.

Recently several groups of investigators have been using the phage-display method to screen for tumor-specific Ags according to a procedure similar to ours (8, 9), but the number of TAAs identified by them was limited, and to the best of our knowledge none converted their clones to complete Abs, which are essential for further studies to try to evaluate their potential therapeutic effects.

## Results

**Isolation of mAbs That Differentially Bound to Cancer Cells.** Using 33 different tumor cell lines from seven carcinomas, hepatocarcinoma, renal carcinoma, pancreatic carcinoma, lung carcinoma, colonic carcinoma, gastric carcinoma, and ovarian carcinoma, the phage Ab library was screened 51 times for isolation of mAbs that bound to molecules present on the cell surface. The number

Author contributions: Y.K. designed research; G.K., Y.A., M.M., M. Sumitomo, N.S., C.M., K.E., K.M., M.T., Y.I., S.H.-T., Y.U., M. Shiraishi, K.S., and M.K. performed research; A.T., S.F., and N.T. contributed new reagents/analytic tools; G.K., Y.A., M.M., A.T., S.F., N.T., R.K., Y.M., M. Shamoto, H.T., M. Sugiura, Y.H., S.M., R.S., K.H., N.H., and A.S. analyzed data; and Y.K. wrote the paper.

The authors declare no conflict of interest.

This article is a PNAS Direct Submission.

Freely available online through the PNAS open access option.

[m]To whom correspondence should be addressed at: Institute for Comprehensive Medical Science, Fujita Health University, 1-98, Dengakugakubo, Kutsukake-cho, Toyoake, Aichi 470-1192, Japan. E-mail: kurosawa@fujita-hu.ac.jp

© 2008 by The National Academy of Sciences of the USA

**Table 1. Summary of screenings**

| Cancer type | Screening no. | Cell | Isolated | Intact | Kinds | Select | Super Select |
|---|---|---|---|---|---|---|---|
| Hepatocarcinoma | 035 | HepG2 | 240 | 162 | 91 | | |
| | 040 | Nuk-1 | 286 | 254 | 100 | | |
| | 041 | OCTH-18 | 239 | 197 | 86 | | |
| | 042 | HepG2 | 96 | 21 | 20 | | |
| | 044 | Hep3B | 190 | 120 | 112 | | |
| | 045 | HepG2 | 428 | 270 | 189 | | |
| | 046 | Clinical sample 0722* | 190 | 156 | 14 | | |
| | 047 | Clinical sample 0722* | 142 | 116 | 18 | | |
| | 048 | Clinical sample 0722* | 142 | 137 | 8 | | |
| | 049 | Clinical sample 0722* | 190 | 160 | 36 | | |
| | 050 | Clinical sample 0722* | 190 | 138 | 51 | | |
| | 051 | HepG2 | 168 | 68 | 49 | | |
| | 052 | HepG2 | 208 | 187 | 94 | | |
| | 053 | HepG2 | 208 | 149 | 71 | | |
| | 063 | HLF | 190 | 141 | 45 | | |
| | 3172 | Clinical sample 0317† | 1 | 1 | 1 | | |
| | 054 | RBE | 250 | 204 | 106 | | |
| | Total | 17 | 3,358 | 2,481 | 1,091 | 967 | |
| Renal carcinoma | 057 | Caki-1 | 190 | 168 | 90 | | |
| | 059 | CCF-RC1 | 190 | 148 | 80 | | |
| | 061 | Caki-1 | 190 | 146 | 53 | | |
| | 062 | CCF-RC1 | 190 | 140 | 111 | | |
| | 060 | ACHN | 190 | 160 | 97 | | |
| | Total | 5 | 950 | 762 | 431 | 341 | |
| Pancreatic carcinoma | 055 | PANC-1 | 286 | 181 | 62 | | |
| | 058 | MIA PaCa-2 | 190 | 159 | 50 | | |
| | 085 | BxPC-3 | 190 | 145 | 61 | | |
| | 087 | Capan-1 | 190 | 44 | 27 | | |
| | Total | 4 | 856 | 529 | 200 | 180 | |
| Lung carcinoma | 064 | A549 | 189 | 172 | 56 | | |
| | 065 | PC-14 | 379 | 349 | 60 | | |
| | 066 | NCI-H441 | 190 | 167 | 71 | | |
| | 068 | Calu-3 | 48 | 34 | 22 | | |
| | 067 | EBC-1 | 285 | 210 | 107 | | |
| | 079 | RERF-LC-AI | 190 | 172 | 73 | | |
| | 080 | LK-2 | 190 | 158 | 86 | | |
| | 086 | VMRC-LCP | 190 | 177 | 69 | | |
| | Total | 8 | 1,661 | 1,439 | 544 | 437 | |
| Colonic cancer | 028 | Caco-2 | 190 | 170 | 102 | | |
| | 029 | CW-2 | 190 | 153 | 92 | | |
| | 082 | SW480 | 190 | 175 | 46 | | |
| | 084 | HT-29 | 190 | 177 | 70 | | |
| | Total | 4 | 760 | 675 | 310 | 279 | |
| Gastric cancer | 031 | MKN-45 | 190 | 159 | 90 | | |
| | 075 | NCI-N87 | 190 | 145 | 50 | | |
| | 077 | SNU-5 | 190 | 143 | 65 | | |
| | 081 | KATO III | 190 | 162 | 79 | | |
| | Total | 4 | 760 | 609 | 284 | 240 | |
| Ovarian cancer | 015 | SKOv3 | 240 | 183 | 81 | | |
| | 021 | SKOv3 | 48 | 10 | 9 | | |
| | 022 | SKOv3 | 48 | 15 | 10 | | |
| | 025 | SKOv3 | 48 | 10 | 6 | | |
| | 026 | SKOv3 | 48 | 20 | 8 | | |
| | 039 | SKOv3 | 48 | 43 | 36 | | |
| | 074 | KF28 | 190 | 143 | 60 | | |
| | 076 | RMG-1 | 190 | 177 | 76 | | |
| | 078 | RMG-2 | 190 | 176 | 79 | | |
| | Total | 9 | 1,050 | 777 | 365 | 287 | |
| Total | | 51 | 9,395 | 7,272 | 3,225 | 2,731 | 2,114 |

*Clinical sample 0722 was derived from a male patient with hepato cell carcinoma HCV (+) stage II.
†Clinical sample 0317 was derived from a male patient with hepato cell carcinoma HBV (+) stage IV-B.

of clones that were picked up in each screening is indicated in the column "Isolated" in Table 1. A total of 9,395 clones were picked up. Those clones were then screened by ELISA using anti-cp3 Ab to examine expression of the intact single-chain Fv (scFv) molecules on the phage because scFv fused with a truncated cp3 was expressed in our system. The number of clones that were

judged to express the intact molecule is indicated in the column "Intact" in Table 1. A total of 7,272 clones turned out to express intact scFv molecules on the phage. Each one of those 7,272 clones was sequenced. The number of clones with different sequences isolated in respective screenings is indicated in the column "Kinds" in Table 1. Because the same clones were redundantly isolated from different screenings, the total number of different clones against the same carcinoma is shown in the column "Select" in Table 1. Because the same clones were also isolated from screenings against different types of carcinoma, 7,272 clones were composed of 2,114 different clones indicated as "Super Select" in Table 1. Of those 2,114 clones 406 were redundantly present in the 3,225 clones summed up in the column "Kinds" in Table 1, and 1,708 were isolated only once in all of the 51-time screenings performed in the present work. The number of times such redundant clones were isolated ranged from two to 27.

Those 2,114 mAbs were individually screened using at least three different fresh tumor tissues for each assay. They were classified into four groups based on the immunostaining patterns in the histological sections. When mAbs significantly stained only the surface of tumor cells but negatively or very weakly stained the other normal cells, they were classified to group A. When the strong staining by mAbs was localized on the surface of malignant cells but a part of the other normal tissue was also stained, they were classified to group B. When mAbs showed positive staining patterns both on malignant cells and on normal cells nonspecifically, they were classified into group C. The clones that did not give any positive signal were classified into group D. Of 2,114 mAbs 281 were classified to group A and 384 were classified to group B.

**Identification of 21 TAAs.** Of the 665 clones, 300 that strongly stained the malignant cells were chosen for further studies. Each of the 300 clones was screened against six different tumor cell lines by using flow cytometry (FCM). They were grouped according to their staining pattern on the basis of the following principle. In FCM analysis, the degree of peak shift should reflect the amount of Ag, the accessibility of Ab, and the strength of binding. The width and shape of peak should reflect the degree of homogeneity of expressed Ags in the cell population. Therefore, if the staining patterns against the six cell lines were identical or very similar among the clones examined, they were grouped together. It led to 40 groups made up of 150 clones. The other 150 clones could not be grouped because of a weak signal in the FCM.

The cell membrane proteins of carcinoma-derived cell lines were biotinylated and then individually immunoprecipitated by the mAbs of the same group and analyzed by SDS/PAGE. When several mAbs in each group gave rise to the same band on the gel the bands were cut out and subjected to MS analysis. This enabled us to identify 21 distinct membrane Ags, which are listed in Table 2. Those 21 Ags are recognized by 84 of the 300 mAbs that we studied.

We also synthesized the extracellular portions of nine of the 21 Ags. Using ELISA we tested the 2,114 mAb clones against those nine synthetic Ags. Of those, 272 clones gave a positive reading in addition to the 84 clones that had been already identified by the MS analysis. We are now in the process of synthesizing the remaining 12 Ags for further screening. To date 356 clones of the 2,114 mAbs isolated in the present study were revealed to specifically bind to one of the 21 TAAs. Of those 356 clones 156 belonged to the redundantly isolated 406 mAbs.

**Expression of Fresh Cancer Tissues.** Using representative clones that specifically bound to 18 TAAs except for three TAAs PTK7, CD9, and CDCP1, which were recently identified, the immunostaining analysis was performed against 24 fresh lung carcinomas. Table 3 summarizes the results of eight TAAs that gave simple patterns showing one of the following two cases: +, overexpression on malignant cells but no or very weak expression on the other normal cells; and −, no expression on either malignant or normal cells. In the case of the other 10 TAAs, although differential expression on malignant cells was distinct, expression on a part of the normal tissue was also observed. From these analyses we concluded the following. (*i*) TAAs identified in our study were overexpressed in fresh tumors at some frequency, but there is no TAA that was overexpressed in all of the fresh tumors. (*ii*) All of the fresh malignant cells analyzed to date overexpressed some of 18 TAAs in various combinations. (*iii*) Approximately half of them showed distinct tumor-specific expression pattern.

**Table 2. Cell-surface Ags identified by the mAbs**

| Ag | MS* | ELISA† |
|---|---|---|
| Growth factor receptor | | |
| EGFR | 3 | 6 |
| HER2 | 1 | 15 |
| HGFR | 3 | 84 |
| PTK7/CCK-4 | 1 | ND |
| Transmembrane protein-tyrosine phosphatase | | |
| PTP-LAR | 5 | ND |
| Adhesion molecule | | |
| Ig superfamily | | |
| IGSF4 | 10 | 13 |
| ALCAM | 3 | 8 |
| ICAM-1 | 5 | 17 |
| Lu/BCAM | 1 | 48 |
| CEACAM6 | 1 | ND |
| Non-Ig family | | |
| CD44 | 3 | ND |
| EpCAM | 2 | ND |
| Tetraspanin | | |
| CD9 | 1 | ND |
| Adenosine metabolism | | |
| Ecto-5′-nucleotidase | 1 | ND |
| Complement inhibitor | | |
| MCP | 8 | 81 |
| Protease inducer | | |
| EMMPRIN | 1 | 0 |
| Iron metabolism | | |
| TfR | 6 | ND |
| Anoikis regulator | | |
| CDCP1 | 2 | ND |
| Integrin family | | |
| $\alpha 3\beta 1$ | 14 | ND |
| $\alpha v\beta 3$ | 8 | ND |
| $\alpha 6\beta 4$ | 5 | ND |

*Number indicates that of different clones identified by MS analysis.
†Clones identified by MS analysis are not included.

**Antitumor Activity of Complete Human IgG mAbs.** After preparing $IgG_1$ mAbs we performed an *in vitro* assay for Ab-dependent cell-mediated cytotoxicity (ADCC) using 22 clones against 10 Ags (EGFR, ALCAM, ICAM-1, EpCAM, HGFR, TfR, ITGA3, EMMPRIN, PTP-LAR, and CD44) using the cell lines listed in Table 4. As can be seen, those mAbs gave a positive reading that ranged between 5% and 95% for cell killing. The details using anti-EGFR Abs and anti-EpCAM Ab are in Fig. 1 *a* and *e*, respectively. The degree of ADCC by clone 059-152 was strong compared with that by cetuximab. Clone 067-153 showed ADCC activity even at an extremely low concentration such as lower than picomolar. We also performed an *in vivo* assay using three

**Table 3. Hisotological analysis of lung carcinomas with mAbs against TAAs**

| | | A | | | B | C | D | | | | | | | | | | | E | | | | | | |
|---|---|---|---|---|---|---|---|---|---|---|---|---|---|---|---|---|---|---|---|---|---|---|---|---|
| Clinical sample | | 1 | 2 | 3 | 4 | 5 | 6 | 7 | 8 | 9 | 10 | 11 | 12 | 13 | 14 | 15 | 16 | 17 | 18 | 19 | 20 | 21 | 22 | 23 | 24 |
| Antigen | Stage Clone Ab | IA | IA | IIIB | IB | IIIB | IA | IA | IA | IB | IB | IB | IB | IB | IIB | IIIA | IIIA | IIIB | IB | IIB | IIIA | IIIA | IIIA | IIIB | IIIB |
| ITGA6 | 029-023 | − | − | − | − | + | − | − | + | − | − | − | − | − | − | + | − | − | − | − | − | − | − | − | − |
| ITGAV | 064-139 | − | + | − | + | + | − | + | − | − | − | − | − | − | − | − | + | − | + | − | − | − | − | − | − |
| CD147 | 059-053 | − | − | − | − | − | + | − | − | − | − | − | − | − | + | + | − | + | + | − | + | + | − | − | + |
| LAR | 064-044 | + | − | + | − | − | − | − | − | − | − | − | − | − | + | − | − | − | − | − | + | − | − | + | − |
| IgSF4 | 076-048 | − | − | − | − | + | + | − | − | + | + | − | + | − | − | − | − | + | − | − | − | − | + | − | − |
| EGFR | 048-006 | + | + | − | + | − | + | + | + | + | + | + | + | − | + | + | + | + | + | + | + | − | + | − | − |
| HER2 | 015-126 | − | − | − | + | − | + | + | − | − | − | − | − | + | + | + | + | + | − | + | + | − | − | − | − |
| HGFR | 067-133 | − | − | − | − | − | + | − | − | − | − | − | − | − | − | − | − | + | − | − | − | − | − | − | − |

A, squamous cell carcinoma; B, adenosquamous carcinoma; C, bronchioloalveolar carcinoma; D, adenocarcinoma; E, large-cell carcinoma.

mAbs against two of the Ags (EGFR and EpCAM) in cancer-bearing athymic mice. As can be seen in Fig. 1*d* the anti-EGFR Abs showed a strong antitumor activity against tumor cell line A431. When we compared our mAbs (048-006 and 059-152) against EGFR with cetuximab it appeared that they had a very similar level of antitumor activity. The anti-EpCAM Ab also prevented the growth of HT29 (Fig. 1*f*).

The two anti-EGFR mAbs were used to analyze the mechanism of their antitumor activities. As can be seen in Fig. 1*b* mAb 048-006 was very effective in inhibiting the binding of EGF to the EGFR, whereas mAb 059-152 only partially prevented the binding reaction. The phosphorylation assay (Fig. 1*c*) showed that mAb 048-006 was effective in the inhibition of phosphorylation. The mAb 059-152 also gave inhibitory effects on phosphorylation, although less effective than 048-006. It suggests that mechanisms of antitumor activity mediated by these two mAbs might be different from each other.

## Discussion

In the present study we used a phage Ab library that had been constructed from human B cells (10). It has been suspected that majority of the clones isolated from phage Ab libraries may not show high affinity to the Ags because they should be naïve to the Ags (11). However, as shown in Fig. 1 two anti-EGFR Abs and one anti-EpCAM Ab showed strong ADCC activity at the concentration of 0.01–0.1 μg/ml, which corresponds to 0.06–0.6 nM. This strength appeared to be practically strong enough to be therapeutic agents whereas comparison of nucleotide sequences of $V_H$ genes encoding theses three Abs with those of germ-line genes indicated that mutations had not been introduced (data not shown). In the screenings of Ab library there were many cases where the same clones were redundantly isolated from different screenings against the same carcinoma as well as against different types of carcinoma. The reason why specific clones were redundantly isolated might be as follows: (*i*) amounts of Ags recognized by them were relatively abundant on the cells used in the screenings, and (*ii*) the binding activity to the Ags was stronger than that of other clones. This interpretation could be at least partly correct. For example, while anti-EGFR Ab 048-006 was isolated by six time screenings the dissociation constant ($K_d$) of the Ag/Ab complex measured by the BIAcore instrument was 0.025 nM (data not shown).

**Table 4. ADCC activities of mAbs that have been converted to IgG**

| Ag | Clone | Target cells | Cell killing,* % |
|---|---|---|---|
| EGFR | 048-006 | NCI-H1373, CCF-RC1, A431, ACHN | 36–80 |
| | 055-147 | CCF-RC1, HT-29, A431 | 25–95 |
| | 059-152 | NCI-H1373, CCF-RC1, A431, ACHN | 35–75 |
| | 059-173 | CCF-RC1, HT-29, A431 | 35–85 |
| ALCAM | 035-234 | NCI-H1373, SKOv3, CW-2 | 8–19 |
| | 041-118 | NCI-H1373, EBC-1 | 14–18 |
| | 066-174 | NCI-H1373, SKOv3, CW-2 | 45–59 |
| | 083-040 | NCI-H1373 | 10 |
| ICAM1 | 053-042 | NCI-H1373 | 16 |
| | 053-051 | NCI-H1373, NCI-H441, HepG2 | 5–31 |
| | 053-059 | NCI-H1373, NCI-H441, HepG2 | 8–39 |
| | 053-085 | NCI-H1373, NCI-H441, HepG2 | 7–26 |
| EpCAM | 067-153 | NCI-H1373, MKN45, HT-29, EBC-1 | 23–80 |
| HGFR | 067-133 | NCI-H1373, MKN45, EBC-1 | 19–42 |
| TfR | 028-178 | MIA Paca2 | 65 |
| | 052-138 | MIA Paca2 | 80 |
| | 041-288 | MIA Paca2 | 30 |
| ITGA3 | 015-003 | ACHN | 20 |
| EMMPRIN | 059-053 | CCF-RC1, ACHN | 40 |
| PTP-LAR | 064-044 | PC14 | 10 |
| | 079-085 | PC14 | 32 |
| CD44 | 064-003 | PC14 | 84 |

*Percentage of cell killing increased dose-dependently. When it reached plateau, the percentage for cell killing was indicated.

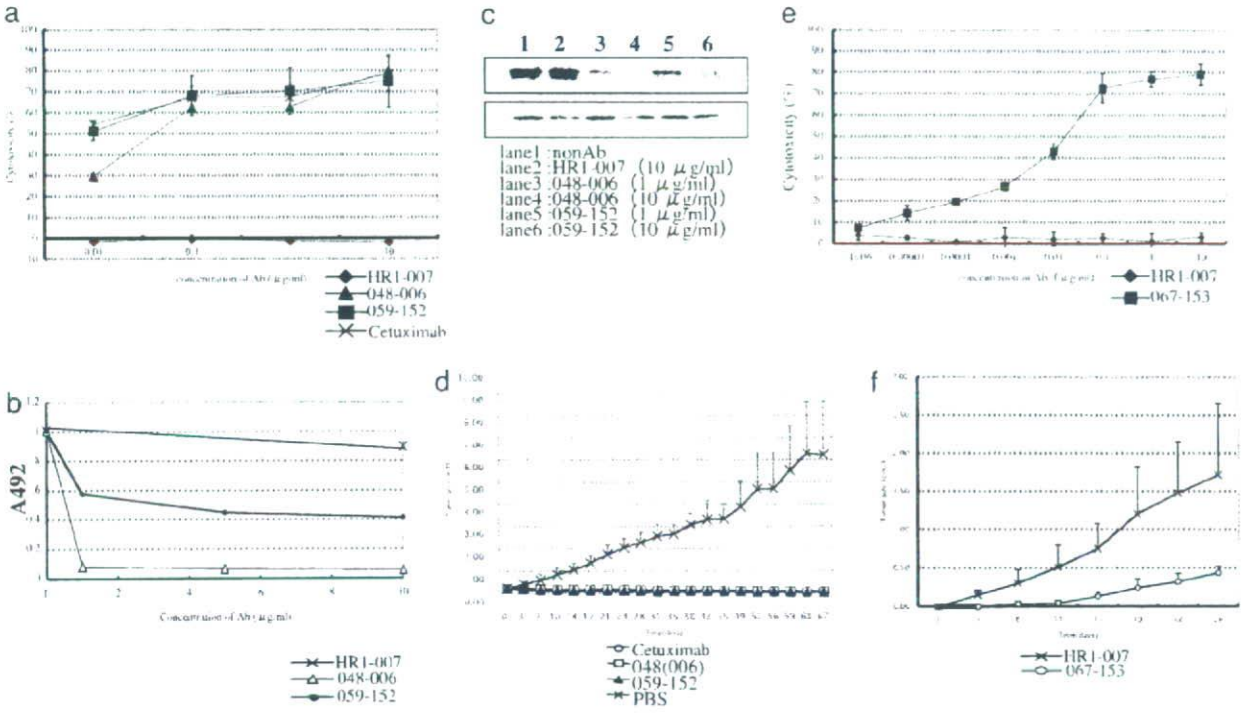


Fig. 1. Antitumor activities of two anti-EGFR mAbs (clone 048-006 and clone 059-152) and an anti-EpCAM mAb (clone 067-153). (*a*) ADCC. Target cells: NCI-1373. Ab: HR1-007 (negative control), mAb 048-006, 059-152, and cetuximab (positive control). (*b*) Inhibitory effects of mAbs on the binding of EGF to EGFR on cell line A431. Ab: HR1-007 (negative control), mAb 048-006, and 059-152. (*c*) Inhibitory effects of mAbs on phosphorylation of EGFR induced by EGF. Upper bands: Western blot by anti phosphotyrosine mouse mAb. Lanes 1–6: incubated for 30 min after addition of EGF at 1 μg/ml; lane 1, without Ab; lanes 2–6, incubated with Ab for 30 min, then EGF was added; lane 2, HR1-007 (negative control) at 10 μg/ml; lanes 3 and 4, 048-006; lanes 5 and 6, 059-152; lanes 3 and 5, 1 μg/ml; lanes 4 and 6, 10 μg/ml. Lower bands: control Western blot with rabbit antiserum against β-actin. (*d*) Inhibitory effects of mAbs on the growth of tumor cell line A431 in athymic nude mice assayed by the first method described in *Antitumor Activity in Vivo*. Ab: HR1-007 (negative control), mAb 048-006, 059-152, and cetuximab. (*e*) ADCC. Target cells: HT-29. Ab: HR1-007 (negative control) and mAb 067-153. (*f*) Inhibitory effects of mAb on the growth of a tumor cell line in athymic nude mice assayed by the alternative method described in *Materials and Methods*. Ab: HR1-007 (negative control) and mAb 067-153.

In this study we isolated 2,114 mAbs with unique sequences that bound to molecules on the surface of tumor-derived cells and selected 665 clones that gave tumor-specific immunostaining patterns. To identify TAAs recognized by the tumor-specific mAbs we developed two strategies. The grouping of mAbs by FCM enabled us to achieve efficient identification of TAAs by the following reasons. (*i*) FCM analyses against several cell lines taught us which cell expressed most abundantly the target molecules. (*ii*) Because multiple mAbs in each group turned out to bind to the same Ag in most cases, many clones have been treated very efficiently by a limited number of experiments. (*iii*) Detergent for solubilization of membrane proteins may destroy the structural integrity with the results of losing the antigenic structure. When several clones classified into the same group were analyzed together, some of them could bind to a relatively detergent-resistant epitope. Screenings of all of the 2,114 mAbs by ELISA with the polypeptides that correspond to the extracellular portions of the TAAs already identified by MS analysis also enabled us to efficiently identify the Ags recognized by respective Abs. Now it is likely that we have already revealed more than half of TAAs potentially identified according to this procedure.

We characterized two anti-EGFR mAbs, clone 048-006 and clone 059-152. Whereas clone 048-006 inhibited both the binding of EGF to EGFR and the phosphorylation of EGFR, clone 059-152 partly inhibited the binding of EGF to EGFR and gave inhibitory effects on the phosphorylation of EGFR less effectively. However, both clones showed a strong antitumor activity in cancer-bearing athymic mice. The characteristics of clone 048-006 appeared to be similar to that of cetuximab (12). However, to the best of our knowledge there has been no report describing mAb whose characteristics was similar to that of 059-152. In the present study multiple Abs have been isolated against respective TAAs. It is possible that these mAbs may have various characteristics as shown by anti-EGFR mAbs.

As indicated in Table 3, half of the TAAs identified in this study gave a tumor-specific staining pattern that is overexpression on malignant cells but no or very weak expression on the other normal cells in the histological sections. These TAAs could be candidates to be useful targets for therapeutic Abs. Furthermore, as indicated in Table 4 and Fig. 1, IgG form of mAbs that bound to them showed strong antitumor activity *in vitro* and *in vivo*. Therefore, we believe that some Ags detected will be useful targets for cancer therapy and that several mAbs will become useful therapeutic agents in the foreseeable future.

## Materials and Methods

**Ab Library and Screening.** AIMS-5 library constructed by using a phage-display system was employed (10). Screenings were performed by a method similar to the one developed by Giordano *et al.* (13). In brief, the phages ($2 \times 10^{13}$ cfu) were mixed with cells ($0.2–1 \times 10^{8}$) in 1.6 ml of solution A (1% BSA, MEM, and 0.1% $NaN_3$), and Ag–Ab complexes on the cell surface were formed. The cell and phage suspension was overlaid on the organic solution in an Eppendorf tube. After the tube was centrifuged, water and organic layers were discarded. The collected cells were suspended in solution A. This process was repeated three times. Finally, the cells were suspended in PBS and frozen in liquid nitrogen. The frozen cells were thawed and mixed with *Escherichia coli*

DH12S. The phages were prepared. This screening round was performed repeatedly three times. After three rounds of screenings, *E. coli* DH12S infected with recovered phages was spread on plates. Approximately 200 colonies were picked up. Thirty-three cancer cell lines listed in Table 1 were used as Ags.

**Immunostaining of Fresh Tumors.** Tumor tissues and the neighboring normal tissues resected by operation were used for immunostaining. They were fixed with 4% paraformaldehyde in 0.1 M cacodylic buffer (pH 7.4) by microwave irradiation as described previously (14).

**Identification of Ag.** Membrane protein analysis was performed according to Zhao *et al.* (15). Proteins present on the cell surface were biotinylated according to the manufacturer's instruction by using the EZ-Link Sulfo-NH-LC Biotinylation kit (Pierce). After the cells were homogenized with a Dounce homogenizer, the protein–membrane complexes were banded between 0.25 M and 1.25 M sucrose layers by centrifugation. The complexes were dissolved in a detergent mixture: 50 mM Hepes (pH 7.6), 150 mM NaCl, 5 mM EDTA, 1% Triton X-100, and 1% $\beta$ octyl glucoside. scFv-$C_L$ fused with cp3 was converted to scFv-$C_L$ fused with protein A domains (scFv-$C_L$-PP) (16). scFv-PP form was covalently bound to beads that were CNBr-activated Sepharose 4B (GE Health Care Bioscience). Ab-bound beads were used for immunoprecipitation as described by David *et al.* (17). MS analysis was performed according to Geuijen *et al.* (8).

**Preparation of $IgG_1$.** ScFv was converted to $IgG_1$ and prepared by using a high level expression vector (18). Using $IgG_1$ mAbs we examined ADCC, effects on binding of EGF to EGFR, effects on phosphorylation of EGFR, and antitumor activity in athymic nude mice.

**ADCC.** The enzymatic activity of lactic dehydrogenase released from the target cells was measured for estimation of ADCC (19). Various cell lines were used as targets for the mAbs. Cells were derived from the following cancers: NCI-H1373, lung adenocarcinoma; CCF-RC1, renal clear cell carcinoma; A431, vulva epidermoid carcinoma; ACHN, renal adenocarcinoma; HT-29, colorectal adenocarcinoma; SKOv3, ovarian adenocarcinoma; CW-2, colorectal adenocarcinoma; EBC-1, lung squamous cell carcinoma; NCI-H441, lung papillary adenocarcinoma; HepG2, hepatocellular carcinoma; MKN45, gastric adenocarcinoma; MIAPaca-2, pancreatic carcinoma; PC14, ling carcinoma. Effector cells were prepared from blood of healthy volunteers and used in a ratio of 100:1 ($10^6$ to $10^4$ in 200 $\mu$l) (20).

**Effects of Anti-EGFR mAbs on the Function of EGFR.** Binding of EGF to EGFR on the cell surface was estimated according to Yang *et al.* (21). Phosphorylation of EGFR induced by EGF was measured according to Matar *et al.* (22).

**Antitumor Activity *in Vivo*.** Two different methods were adopted. In the first method each mouse was injected with $5 \times 10^6$ cells, and when the tumor grew to 0.2 $cm^3$ mAb therapy was initiated. Treatments consisted of twice-weekly i.p. injections of mAb for 3 weeks. One milligram in 0.5 ml of PBS was used in each injection. Control animals received injection of PBS. Six mice were used for each treatment. The alternative method: 1 day after injection of cells mAb therapy was started. Treatments consisted of twice-weekly i.v. injections of mAb for 2 weeks. A total of 50 $\mu$g was used in each injection.

**ACKNOWLEDGMENTS.** This work was supported in part by a grant-in-aid for the 21st Century Center of Excellence Program of Fujita Health University from the Ministry of Education, Culture, Sports, Science, and Technology and by a grant from the New Energy and Industrial Technology Development Organization (to Y.K.).

1. Waldmann H, *et al.* (1984) Elimination of graft-versus-host disease by in-vitro depletion of alloreactive lymphocytes with a monoclonal rat anti-human lymphocyte antibody (CAMPATH-1). *Lancet* ii:483–486.
2. Carter P, *et al.* (1992) Humanization of an anti-p185HER2 antibody for human cancer therapy. *Proc Natl Acad Sci USA* 89:4285–4289.
3. Reff ME, *et al.* (1994) Depletion of B cells in vivo by a chimeric mouse human monoclonal antibody to CD20. *Blood* 83:435–445.
4. Adams GP, Weiner LM (2005) Monoclonal antibody therapy of cancer. *Nat Biotechnol* 23:1147–1157.
5. Okabe H, *et al.* (2001) Genome-wide analysis of gene expression in human hepatocellular carcinomas using cDNA microarray: Identification of genes involved in viral carcinogenesis and tumor expression. *Cancer Res.* 61:2129–2137.
6. Hippo Y, *et al.* (2002) Global gene expression analysis of gastric cancer by oligonucleotide microarrays. *Cancer Res* 62:233–240.
7. Winter G, Griffiths AD, Hawkins RE, Hoogenboom HR (1994) Making antibodies by phage display technology. *Annu Rev Immunol* 12:433–455.
8. Geuijen CAW, *et al.* (2005) A proteomic approach to tumour target identification using phage display, affinity purification and mass spectrometry. *Eur J Cancer* 41:178–187.
9. Goenaga AL, *et al.* (2007) Identification and characterization of tumor antigens by using antibody phage display and intrabody strategies. *Mol Immunol* 44:3777–3788.
10. Morino K, *et al.* (2001) Antibody fusions with fluorescent proteins: A versatile reagent for a profiling protein expression. *J Immunol Methods* 257:175–184.
11. Ghorardi E, Milstein C (1992) Original and artificial antibodies. *Nature* 357:201–202.
12. Goldstein NI, Prewett M, Zuklys K, Rockwell P, Mendelsohn J (1995) Biological efficacy of a chimeric antibody to the epidermal growth factor in a human tumor xenograft model. *Clin Cancer Res* 1:1311–1318.
13. Giordano RJ, Cardo-Vila M, Lahdenranta J, Pasqualini R, Arap W (2001) Biopanning and rapid analysis of selective interactive ligands. *Nat Med* 7:1249–1253.
14. Mizuhira V, Hasegawa H (1997) Microwave fixation and localization of calcium in synaptic terminals using X-ray microanalysis (EDX) and electron energy loss spectroscopy (EELS) imaging methods. *Brain Res Bull* 43:53–58.
15. Zhao Y, Zhang W, Kho Y, Zhao Y (2004) Proteomic analysis of integral plasma membrane proteins. *Anal Chem* 76:1817–1823.
16. Ito W, Kurosawa Y (1993) Development of an artificial antibody system with multiple valency using an Fv fragment fused with a fragment of protein A. *J Biol Chem* 268:20668–20675.
17. David GS, Chino TH, Reisfeld RA (1974) Binding of proteins to CNBr-activated sepharose 4B. *FEBS Lett* 43:264–266.
18. Bebbington CR, *et al.* (1992) High-level expression of a recombinant antibody from myeloma cells using a glutamine synthetase gene as an amplifiable selection marker. *Biol/Technology* 10:169–175.
19. Decker T, Lohmann-Matthes ML (1988) A quick and simple method for the quantitation of lactose dehydrogenase release in measurements of cellular cytotoxicity and tumor necrosis factor (TNF) activity. *J Immunol Methods* 115:61–69.
20. Boeyum A (1964) Separation of white blood cells. *Nature* 204:793–794.
21. Yang XD, *et al.* (1999) Eradication of established tumors by a fully human monoclonal antibody to the epidermal growth factor receptor without concomitant chemotherapy. *Cancer Res* 59:1236–1243.
22. Matar P, *et al.* (2004) Combined epidermal growth factor receptor targeting with the tyrosine kinase inhibitor gefitinib (ZD1839) and the monoclonal antibody cetuximab (IMC-C225): Superiority over single-agent receptor targeting. *Clin Cancer Res* 10:6487–6501.

Trends in Cancer Research
Vol. 3, 2007

Review

# Rat mammary preneoplasia and neoplasia: a model for human breast cancer research

**Yoichiro Matsuoka[1,*], Hiroaki Kawaguchi[2], Hiroki Yoshida[2], Hiroyuki Tsuda[3] and Airo Tsubura[1]**

[1]Second Department of Pathology, Kansai Medical University, 10-15 Fumizono-cho, Moriguchi, Osaka 570-8506, Japan. [2]Department of Tumor Pathology, Field of Oncology, Kagoshima University Graduate School of Medical and Dental Sciences, 8-35-1 Sakuragaoka, Kagoshima 890-8544, Japan. [3]Department of Molecular Toxicology, Nagoya City University Graduate School of Medical Sciences, Mizuho-cho, Mizuho-ku, Nagoya 467-8601, Japan

## ABSTRACT

An experimental system that biologically and histologically mimics human breast cancer is needed to understand the pathogenesis of the disease and to build strategies for its prevention and cure. The experimental system should be a tool to assess the influence of host factors, such as age, reproductive history, and genetic background, as well as environmental factors. Rat mammary gland carcinogenesis is the model that most closely fulfills these conditions.

**KEYWORDS:** carcinogenesis, experimental model, mammary carcinoma, preneoplasia, rat

## INTRODUCTION

Breast cancer remains the most frequent type of cancer in women worldwide. The incidence of breast cancer in Western countries is leveling off and may have recently started to decline, especially in women younger than 40 years [1]. However, the incidence of this disease is definitely increasing throughout Asia.

A possible genetic contribution to breast cancer risk is indicated by the increased incidence of breast cancer among women with a family history of breast cancer and by the observation of families in which multiple family members develop breast cancer. Other risk factors for breast cancer include: age, previous breast disease, reproductive and menstrual history, estrogen therapy, radiation exposure, diet, and alcohol intake. While many epidemiological studies have addressed the effects of these risk factors in women, an experimental system that closely mimics human breast cancer is needed to directly investigate the factors that contribute to breast cancer risk. The rat mammary gland treated with carcinogens is one of the most widely studied and useful models of mammary carcinogenesis. In this review, we describe the development of rat mammary glands, induction and pathogenesis of the mammary tumors, and utility of the induced tumors for human breast cancer research.

*Corresponding author
matsuoyo@takii.kmu.ac.jp

### Development of rat mammary gland

The proliferation and differentiation of the mammary gland involves a variety of hormones and growth factors, such as estrogen, progesterone, prolactin, hepatocyte growth factor, growth hormone, and IGF-1 [2-4]. The functional and structural development of the gland itself can be divided into seven stages: embryonic, postnatal, juvenile, puberty, pregnancy, lactation, and involution.

#### Embryonic stage

By day 11 of gestation, two parallel ridges of ectoderm lateral to the midline extend from the